AD

Research and Development Technical Report

ECOM-C-0423-6

WIND TUNNEL STUDIES OF THE AIR FLOW AND GASEOUS PLUME DIFFUSION IN THE LEADING EDGE AND DOWNSTREAM REGIONS OF A MODEL FOREST

TASK IIB RESEARCH TECHNICAL REPORT

DESERET TEST CENTER

By

R. N. MERONEY

and

B. T. YANG

NOVEMBER 1969

ECOM

UNITED STATES ARMY ELECTRONICS COMMAND
ATMOSPHERIC SCIENCES LABORATORY
FORT HUACHUCA, ARIZONA
CONTRACT DAAB07-68-C-0423
COLORADO STATE UNIVERSITY, FORT COLLINS 80521

CER69-70RNM-BTY-17

DISCLAIMER

Technical Report ECOM C-0423-6
November 1969

Reports Control Symbol
OSD-1366

Wind Tunnel Studies and Simulations of Turbulent Shear Flows Related to Atmospheric Science and Associated Technologies

TECHNICAL REPORT

WIND TUNNEL STUDIES OF THE AIR FLOW AND GASEOUS PLUME DIFFUSION IN THE LEADING EDGE AND DOWNSTREAM REGIONS OF A MODEL FOREST

DA Task 1T061102B53A-17

PREPARED BY

R. N. MERONEY

and

B. T. YANG

Fluid Dynamics and Diffusion Laboratory
Fluid Mechanics Program
College of Engineering
Colorado State University
Fort Collins, Colorado
80521

for
ATMOSPHERIC SCIENCES LABORATORY
U. S. Army Electronics Command

Fort Huachuca, Arizona

CER69-70RNM-BTY-17

ABSTRACT

A model forest canopy was designed to simulate the meteorological characteristics of typical live forests. Measurements were made of velocity, turbulence, drag, and gaseous plume behavior. Flow properties are compared with recent field measurements. Ground penetration in the initial fetch region results in strikingly different streamline motion as compared to wind motions within the equilibrium regions. Measured values of the vertical eddy diffusion coefficient are shown to predict plume behavior in the equilibrium region very well if a correction is included for the ratio $\frac{K_y}{K_z} > 1.0$.

Ventilation of an elevated line source into the canopy region is compared with a simple one-dimensional model.

TABLE OF CONTENTS

LIST OF FIGURES

LIST OF FIGURES (continued)

LIST OF TABLES

WIND TUNNEL STUDIES OF THE AIR FLOW AND GASEOUS PLUME DIFFUSION IN THE LEADING EDGE AND DOWNSTREAM REGIONS OF A MODEL FOREST

by

R. N. Meroney* and B. T. Yang**

1. INTRODUCTION

Wind movement within forest stands and in their boundary regions dominates the exchange processes which occur within the vegetative canopy. The structure of the timber stand interacts with the prevailing winds to determine fire spread rates, snow pack, soil erosion, dispersal of seed for forest regeneration, blow down, and rates of carbon dioxide and water vapor exchange during plant metabolism.

As early as 1893, Metzger, a German scientist, investigated the effects of wind action on trees. Subsequently, a variety of studies have been made of the behavior of winds well inside a forest (Bayton, 1963; Cooper, 1965; Denmead, 1964; Fons, 1940; Huston, 1964; Poppendiek, 1949; Tiren, 1927; Tourin and Shen, 1966). Some measurements are available for the variation of the wind at the edge of a forest (Iizuka, 1952; Reifsnyder, 1955). These measurements have provided a rough picture of a highly complex and turbulent flow field within the vegetative canopy.

Agricultural meteorologists, atmospheric scientists, and many hydrologists are interested in the evaporation and

---

* Assistant Professor of Civil Engineering, Colorado State University
** Graduate Research Assistant, Department of Civil Engineering, Colorado State University

exchange processes which occur in vegetative canopies. Such information permits calculation of the efficiency of water, energy, and CO_2 transport in plant metabolism and the movement of foreign additives into or out of the bulk of a canopy. Since 1937, experimenters have made measurements of velocity, temperature, evaporation rates, and energy balance within and above such configurations (Penman and Long, 1960; Inoue, 1963; Uchijima and Wright, 1964; Lemon, 1962). These measurements have provided a rough picture of a highly complex and turbulent flow field within vegetation.

Past measurements of diffusion from point or line sources in forest configurations seem to have been limited to measurements of an instantaneous line source over a tropical rain forest by Bendix (Baynton, 1963), of point and line source distributions over a deciduous forest by Litton Systems (Tourin and Shen, 1966), of instantaneous point sources in a jungle-like deciduous forest by MELPAR (Allison, et al., 1968), and of rates of particulate dispersion in a forest canopy at Brookhaven (Raynor, 1967, 1969). These measurements are extensive and well documented; however, they must be normalized to some simplified geometry in order to determine the universal characteristics and governing parameters of vegetative penetration by a diffusing plume.

Since field measurements are not easy to obtain because of the cost of providing a perfect measuring station and the difficulty of obtaining cooperative weather, a laboratory program of modeling the flow in and above plant covers has been initiated at the Fluid Dynamics and Diffusion Laboratory at Colorado State University. Previous results from this program have been published by Quarishi and Plate (1965), Meroney and Cermak (1967), and Meroney (1968).

The purpose of this report is to discuss some measurements of diffusion from a continuous point source in and above a model forest canopy. The results of this study will consist of:

1) A description of the diffusion process in and above the simulated canopy;

2) A description of the vertical dispersion of the tracer materials;

3) A determination of the effect of the initial fetch of the forest canopy on tracer dispersion, and finally,

4) A determination of the vertical distribution of the eddy diffusion coefficients in and above the modeled canopy.

2. MODELING OF A FOREST CANOPY

The wind tunnel has been used repeatedly by the forest meteorologist in his effort to understand the complex pattern of flow generated by the tree--a permeable, random shaped, elastic object. Tiren, in 1927, attempted to estimate crown drag from conifer branch-drag measurements made in a wind tunnel as part of his study of stem form. Wind-breaks have been studied by models to determine soil erosion and blow down characteristics.

Researchers have modeled forest behavior using live tree boughs, cotton balls, wooden pegs, plastic strips, and even wire mesh (Hirata, 1953; Iizuka, 1956; Malina, 1941; Woodruff and Zingg, 1952). These studies were all conducted to deduce the qualitative behavior of tree barriers for specific problems. The investigators apparently made no attempt to scale dynamically the character of a live tree except to compensate intuitively for shape and porosity. To model completely the complex geometry and structural characteristics of a live tree is obviously not practical; however, measurements made on coniferous and deciduous trees in the wind tunnel and in the field suggest that equivalence of drag and wake characteristics between model and prototype trees should be sufficient to study the general flow phenomenon (Lai, 1955; Rayner, 1962; Sauer et al., 1951; Walske and Fraser, 1963).

Correlation of the measurements mentioned above plus additional ones made on live trees at Colorado State University indicates that the drag coefficient C_D may vary with wind speed from 1.0-0.3 (Burgy, 1961) (Fig. 5). These measurements indicate that the flow is inertially dominated (i.e., Reynolds number independent), but that self-streamlining of the tree at high velocities can reduce the effective cross-sectional area for the more flexible species.

Measurements made behind small specimens of Colorado spruce, juniper, and pine trees revealed that linear wake growth exists behind all trees, that the wake shadows of individual branches disappear within 1-2 tree crown diameters downstream, and that the velocity defect becomes Gaussian within 3-4 crown diameters (Fig. 6).

After studying a variety of plastic, metal and brush model trees, a model made from plastic simulated-evergreen boughs was selected. The model trees chosen have an average height of 18 cm, a stem height of 5 cm, and a crown diameter of 7 cm. The model tree has a drag coefficient of 0.72 over the velocity range studied and a lateral wake growth similar to that measured for live trees (Figs. 5 and 6).

Results of extensive single tree drag measurements made within regular geometric arrays of the same model tree (an orchard arrangement) are reported by Hsi and Nath (1968). The drag profiles measured show a similar behavior to the bending moment measurements made by Walske and Fraser (1963); that is, there is a sharp decrease in drag on the trees with distance down-wind followed by a slight rise to an asymptotic constant value.

Shear plate measurements made within the random canopy array under discussion herein display the same characteristics as the regular arrangements. Figure (7) plots local shear force vs distance downwind from the canopy inception. The minimum observed within the first 2 m is evidently the result of a relatively stagnant region inside the canopy which also explains the behavior of the diffusion plume discussed subsequently. This same phenomenon was found for flow over a model peg canopy (Meroney and Cermak, 1967).

3. EXPERIMENTAL EQUIPMENT AND PROCEDURES

3.1 Wind Tunnel and Canopy Arrangement: The experimental data were obtained in the low speed Army Meteorological Wind Tunnel in the Fluid Dynamics and Diffusion Laboratory at Colorado State University (Plate and Cermak, 1963). This tunnel was specifically designed to study fluid phenomena of the atmosphere. The tunnel has a 2 m square by 26 m long test section with an adjustable ceiling to provide a zero pressure gradient over the forest canopy. The model trees were inserted into holes in aluminum plate sections which extended the width of the tunnel and 11 m downstream from the tunnel midsection. The elements were randomly positioned with approximately one tree per 36 cm^2. From above, this arrangement gave the same visual appearance as a moderately dense coniferous forest. This density would be equivalent to a stand density index as calculated by Reinke (1933) of 250 for a forest with an average tree height of 40 ft and a diameter at breast height of 10 inches (Fig. 1), (Fig. 2). A volumetric density number has been calculated to describe the canopy density by Sadeh, et al., (1969). When one describes the volume occupied by a single tree as a combination of a crowncone and trunk cylinder, the ratio of tree occupied volume to volume beneath the mean canopy height is 26%.

3.2 Velocity and Turbulence Measurements: A single wire constant temperature anemometer was used to measure velocity, turbulent intensity, and shear. In addition, pitot-static tube measurements were made at each section. The sensing elements of the anemometer circuit were platinum wire 0.2 mil in diameter and approximately 0.25 cm long. The bridge circuit utilized was a CSU Solid State Anemometer. The pitot tube output went to a Transonic Model A, Type 120 electronic pressure meter. Turbulence signals were interpreted by means of a Bruel and Kjaer RMS meter, Model 2416.

3.3 <u>Concentration Measurement-Helium Tracer Gas:</u> The character of the flow field was studied by mapping the diffusion plume of a continuous point source. Helium gas was used as one tracer for the diffusion experiment. The gas was released continuously at a constant rate of 630 cc/min from a 2 mm nozzle located in or above the canopy. The sampling probe, manufactured from small diameter hypodermic tubing, was mounted on a traversing carriage, the horizontal and vertical positions of which were controlled remotely from outside the tunnel. Helium concentration was measured at ground level along a line normal to the axis of the plume and vertically at the plume centerline.

Samples were drawn into the probe at a constant rate and passed over a standard leak into a mass spectrometer (Model MS9AB of the Vacuum Electronic Corporation). Output of the mass spectrometer was an electrical voltage proportional to concentration. The mass spectrometer was calibrated periodically by a set of pre-mixed gases of research grade. Figure 3 shows the experimental arrangement.

Since a closed-circuit wind tunnel was used, the ambient concentration level of helium built up in the wind tunnel with time. Eventually, most of the gas did leak out; therefore the amount of helium in the ambient flow was never higher than 60 parts per million. Nevertheless, an ambient concentration measurement was taken after each profile. The relative concentration was obtained by subtracting the corresponding ambient concentration from the absolute concentration. All data presented in the figures or tables are relative concentrations.

Due to the slow response of the mass spectrometer, a period of one to two minutes was allocated for the stabilization of each reading before it was recorded. Usually, the concentration signal itself was averaged over at least 60 seconds. This method gave results that compared favorable with the average of signals taken over a period as long as 250 seconds by graphical means.

3.4 <u>Concentration Measurement - Kr-85 Tracer Gas:</u> To investigate the buoyancy character of the helium tracer additional measurements were obtained utilizing a mixture of Kr-85 and air as a tracer. It is a radioactive noble gas which does not chemically combine with any other molecules in the system studied. Krypton-85 has a half life of 10.6 years so there is no appreciable decay during a diffusion experiment. The radioactive gas was diluted about a million times before use and, as such, has physical characteristics equivalent to those of air. Its detection procedure is fairly simple and direct. Handling and safety procedures for wind tunnel experiments with Kr-85 tracer gas have been discussed in detail by Chaudhry and Meroney (1969).

The flow rate of Kr-85 mixture was controlled by a pressure regulator at the bottle outlet and monitored by a Fisher and Porter flowmeter. Source concentration was 6.4 μ-curie/cc of Kr-85, a beta emitter.

A sampling rake of eight probes was manufactured from 2 mm diameter hypodermic tubing and was mounted on a traversing carriage whose horizontal and vertical position was controlled remotely from outside the tunnel. Concentrations were measured at ground levels at various scaled distances from 200 to 400 feet downwind and at vertical elevations centered on plume maximum concentrations. Samples were aspirated at a constant rate of 500 cc/min into eight TGC-308 Tracerlab Geiger-Mueller side wall cylindrical counters. Samples were flushed through the counting tubes for at least two minutes, Valve A in Figure (5B) was closed, and each sample was subsequently counted for one minute on Nuclear Chicago Ultra-scaler Model 192A. All samples counted were adjusted for background radiation (See Fig. 4a and 4b).

4. EXPERIMENTAL RESULTS

All measurements were taken at a free stream velocity of 6 m sec^{-1}. The ceiling of the test section was adjusted for zero pressure gradient and the upstream velocity profile was measured and found to be logarithmic. The temperature condition was constant and hence neutral stability existed.

4.1 Typical Velocity and Turbulent Intensity Profile Results:

A sequence of vertical profiles of mean velocity measurements were made along the tunnel centerline both in and above the forest canopy. The transformation of the wind profiles in the vertical direction are shown in Figure (5). Jetting of the wind flow beneath the canopy is observed for at least the first 3 m (or 15 canopy heights); subsequently, the wind profile reaches an equilibrium state at about 4 m (or 20 canopy heights). Finally, accelerations of the wind are observed during the last 2 m of the canopy as the wind adjusts to the smooth surface downwind. The extent of the entrance region agrees with previous measurements by Meroney and Cermak, and Plate and Quarishi (1965), but is greater than that tentatively suggested by Reifsnyder (1955). The shape of the equilibrium velocity profile agrees qualitatively with prototype measurements for moderately dense conifer forests (Cooper, 1965; Denmead, 1964; Fons, 1940; Poppendiek, 1949; Reifsnyder, 1955; Tiren, 1927; Tourin and Shen, 1966).

In the winter the Minnesota deciduous forest of Tourin and Shen (1966), compares favorably quantitatively with a fairly dense peg arrangement (Fig. 10), whereas, the plastic tree canopy simulates summer measurements made by Allen (1968), Shinn (1969), and Tourin and Shen (1966), (Fig. 11).

Velocity data from the plastic tree canopy has also been compared with prototype measurements by means of a dimensionless velocity defect argument. Shinn (1969) calculated the defect between the pre-canopy velocity profiles and that measured within the forest. The result for a fetch length of $x/h = 5$ is displayed in Figure (12).

The profiles above the canopy are logarithmic and can be plotted to follow the displacement law $u/u^* = k^{-1}\ln[(y-d)/z_o]$ as shown by Plate and Quarishi (1965). However, it should be noted that the popular regression technique first suggested by Lettau to solve for u^*, d, and z_o could not be utilized unless modified (Robinson, 1961). This program (a version of which is known as the "Three Bears" program) unfortunately assumes u^*, d, and z_o are independent; as a result, some investigators have obtained the physically suspect result that d is negative (Kung, 1961). In our computations, d was assumed equal to the canopy height; thus $z_o \simeq 22$ cm, and $u^* \simeq 14$ m/sec. In addition, measurements over the peg canopy suggested that the velocity profiles may be dominated by the canopy top wake until $z \simeq 2.5$ to 3 h; hence, it would appear that forest micro-meteorologists should not attempt a log-law analysis unless they utilize fairly tall towers. Moreover, recent analysis of data for above canopy flows suggests that the friction velocity and roughness length are not local quantities but vary with height; perhaps because the assumption of a constant shear stress region is invalid, (Sadeh, et al., 1969).

Hot wire anemometers were used to measure turbulence characteristics in and over the model canopy (Fig. 9). Values of longitudinal intensity up to 0.35 were measured in and above the model forest canopy. They correspond to field measurements by Tourin and Shen (1966) who report average values of longitudinal turbulence of 0.33 at the 40 foot level. Subsequent measurements by (Sadeh, et al., 1969) also measured high turbulence intensity levels; however, changes in measurement techniques resulted in values as high as 0.77 in the established flow regime. Tourin and Shen also noted the decrease of turbulence as one moves downward into the forest cover.

4.2 Diffusion Plume Results: Plumes were released at the model forest entrance from locations near the ground, at half canopy height, and at the top of the canopy. Releases were also made in the equilibrium wind profile region downstream. Tables 1 through 7 summarize data measured.

Figures (13) and (14) display the typical plume exhalation by the forest near the entrance and the subsequent re-inhalation further downstream. A similar behavior has been noticed for releases of gas over a model crop canopy simulated with dowel pegs (Meroney and Cermak, 1967, Yano, 1967). This phenomena is a result of vertical motions near the front of the forest canopy previously reported by Iizuka (1952). The subsequent rapid penetration further downstream may be due to the intense shear and mixing near the canopy top over the initial fetch region. The ramification of this effect upon fire spread and parasite control by spray is obvious.

Plume releases within the forest near the ground were characterized by wide meandering and large lateral dispersal. Such erratic behavior including plume bifurcation occurs frequently during forest diffusion experiments (Allison, 1968; Shinn, 1969; Geiger, 1950).

Figures (15) through (18) present vertical-isoconcentration sections through continuous point source plumes released at various heights above the ground (i.e., 0, 1/2h, h, and 1-1/2h) where the flow field appears fully established (i.e., x/h = 33). For the elevated releases the sequence of stages of the concentration gradient observed upon penetration of the plume downstream are similar to those observed by Flemming (1967) during elevated line source releases over a deciduous forest. Initially, there is a gradient downward followed by a gradient in concentration upward even farther downstream.

It is interesting to note how the diffusing cloud tilts forward near the tree top due to wind shear, and how a rapid forward movement has resulted from the relatively high wind speed at the tree tops. The very rapid vertical growth of the plume for ground source releases is another feature also duplicated by ground based bomblet measurements (Tourin and Shen, 1969). The MELPAR study did not incorporate any significant number of vertical measurements; however, observation of puff behavior led to the conclusion vertical mixing to the canopy top was complete within very short downwind distances (MELPAR, 1968).

It has been generally observed for continuous plume releases that the maximum concentration at ground level decreases at a rate proportional to a power function of the longitudinal downstream distance, x^{-m}. For a plume dispersing in or above a vegetative canopy, the rate of dispersal also appears to be a function of the distance from the release position, $(x-x_s)^{-m}$, (see Fig. 19). The rate of dispersion, however, is much larger than for plumes dispersing over a smooth surface (Malholtra and Cermak, 1964), (i.e., $m_{\substack{\text{canopy}\\\text{plastic}}} = -4.8$, $m_{\substack{\text{peg}\\\text{canopy}}} = -2.5$, $m_{\substack{\text{smooth}\\\text{surface}}} = -1.5$).

Examination of bomblet releases in a deciduous forest by Tourin and Shen (1966) produced values of $m \cong -7.0$ for a typical near-neutral summer release and $m \cong -3.0$ for a winter release. The average decay rate for all F.P. releases in a summer jungle canopy was found to be -3.1 by MELPAR, Inc. (1968).

Brown, et al. (1969) have proposed that the ventilation rate of most vegetative canopies may be correlated to an environmental index defined as $EI = u_{ac.} / u_{bc.}$ where

$u_{a.c.}$ = velocity at two canopy heights.

$u_{b.c.}$ = velocity at one-half canopy heights.

If the coefficient $-m$ is plotted versus such an environmental index one notes an increase in dispersion rate as the index increases followed by a decrease to zero for very dense vegetative configurations. This behavior appears to correlate with the increase in turbulent intensity initially until the blockage becomes so great as to inhibit the rate of disperson of the gases, after which $-m$ decreases, see Figure (26).

When the flow above and below the canopy ceiling are treated as separate flow regimes, similarity conditions appear to exist when the appropriate characteristic length parameters are chosen. If the character of the concentration profile is examined above the canopy top, one finds that similarity may be obtained over long fetch distances by displaying C/C_h vs $(z - h)/(\lambda - h)$; where h = canopy height, and λ = characteristic width of plume when $C = \frac{1}{2} C_h$, (Fig. 20). Data is compared to an analytic expression which also summarized the character of plume releases over smooth surfaces.

Comparison of isoconcentration profiles for the Helium tracer gas and Kr-85 tracer gas suggests that the initial buoyancy of the undiluted Helium source had little effect on the dispersion in and above the canopy. Figures (16a) and (16b) display the measurements for the Helium and Krypton tracers respectively. In addition, slight variations observed in the ground level concentration variation with downward distance are not of the order or direction to be attributed to buoyancy effects.

4.3 Eddy Diffusion Coefficient: The concept of a macroscopic equation of turbulent dispersion of some property C results generally in the equation

$$\frac{\partial C}{\partial t} + \frac{\partial}{\partial x_i} (u_i C) = \frac{\partial}{\partial x_i} \left(K_{x_i} \frac{\partial C}{\partial x_i}\right) \qquad (1)$$

where K_{x_i} is the coefficient of turbulent diffusion. The coefficient K_{x_i} incorporates within itself the complexities of the actual transport process. Hence, most analytical studies of fluid mechanics require some theoretical or empirical expression for the variation of K_{x_i} with other parameters. Several scientists have studied the nature of K_{x_i} for plant communities, but further data are still needed (Penman and Long, 1969; Inoue, 1963; Yano, 1966; Saito, 1964).

The eddy diffusion coefficient for transport of the injected gas in the model canopy has been determined utilizing concentration and velocity profiles and a finite difference interpretation of Equation (1). In order to simplify the discretization analysis the concentration data were converted to line source data by the assumption of normal distributions and lateral integration. Two computational methods were utilized to calculate $K_z(z)$. In one, Equation (1) was solved directly in finite difference form for $K_z(z)$ such that

$$K_z(z) = \frac{u \frac{\partial c}{\partial x} + \frac{K_z(z-2\Delta z) - 4K_z(z-\Delta z)}{2\Delta z} \frac{\partial c}{\partial z}}{\frac{\partial^2 c}{\partial z^2} + \frac{3}{2} \frac{1}{\Delta z} \frac{\partial c}{\partial z}} \qquad (2)$$

where $\frac{\partial c}{\partial x}$, $\frac{\partial c}{\partial z}$, and $\frac{\partial^2 c}{\partial z^2}$ are replaced by their finite difference approximations. In the second method, Equation (1) was integrated once in z to eliminate the second derivative term such that

$$K_z(z) = \frac{\int_0^z u \frac{\partial c}{\partial x} dz}{\left(\frac{\partial c}{\partial z}\right)_z} \quad . \qquad (3)$$

These methods gave essentially identical results in and above the forest canopy. Calculations were performed on a CDC 6400 computer at Colorado State University using input data taken from lines faired through the ground source concentration measurements, at $x_s = 6$ Meters and from vertical velocities calculated from the slope of streamlines.

The resulting profiles in $K(z)$ are displayed in Figure (21). Three distinct regions of variation of K are noticeable. Immediately adjacent to the wall is a zone where K increases exponentially. In the area from 4 to 12 cm, K remains essentially constant; and K becomes proportional to $(z-d)$ where d is a displacement height. Similar behavior has been observed for prototype canopies. Finally, these K profiles may also be described as qualitatively similar to the peg data.

A number of authors have suggested that K should remain constant in vegetative cover; others have suggested that K should vary linearly (Inoue, 1963; Uchijima and Wright, 1964). It is interesting to note that for the case of the model peg canopy, both conditions of K exist, although in different regions. Figure (22) compares the distribution of K within the canopy with typical results of the distribution of K for a pine forest as measured by Denmean, (1964).

The experimental data mesh from which the estimates of $K_z(z)$ were obtained was fairly coarse; hence, to verify the results it was decided to recompute the concentration distributions numerically for the elevated release conditions for a continuous point source situation. Equation (1) was discretized and solved by means of an alternating-direction-implicit technique described by Peaceman and Rachford (1955). Initially it was assumed $K_y \equiv K_z(z)$.

Figure (23) compares the ground concentrations as measured and as calculated when initial plume concentrations at $x = 25$ cm were substituted into the calculation procedure. If a value of the ratio $K_y/K_z = 2.0$ or 4.0 is assumed, one obtains a somewhat better comparison as shown on the same figure. The value of K_y is normally expected to exceed K_z especially in the near ground region. Faster lateral dispersion at ground level has also been observed for model peg canopies (Meroney and Cermak, 1967).

Figure (24) displays the result of the assumption $K_y/K_z \geq 1$ upon the cross-section isoconcentrations lines as seen for an elevated and ground release in the plastic tree canopy.

4.4 Forest Penetration Model: Despite the existence of complex sets of diffusion data in various vegetative canopy configurations, only elementary solutions for understanding physical dispersion of gases in forests has been put forward. Most experimentalists have tried to fit their results to regression equations (Baynton, 1963; Tourin and Shen, 1969; Allison, 1968); for example Baynton (1963) suggested

$$(\text{Dosage})_{\text{ground}} = [A + \frac{B}{10^{C + DU + E\Delta T}}]\,\sigma_\theta\,(\text{Dosage})_{\text{above canopy}};$$

where U is velocity above the canopy, ΔT is temperature difference above and below canopy, and σ_θ is standard deviation of wind direction above forest. As Baynton notes such a formula applies specifically to the forest in which the data were collected since the height of the forest and forest density are not parameters. Baynton could detect no below canopy mean and speed in his dense jungle canopy; hence his regression formula only allows for vertical diffusion in and out of the forest with no longitudinal convection. Tourin and Shen, on the other hand, worked in a somewhat less dense canopy and suggested that the relation

$$\frac{\text{(Dosage) ground}}{Q} = 0.51\ x^{-0.993}\ \vec{\sigma}_\varepsilon^{\ -0.75}\ \bar{u}^{\ -0.98}(1-F)^{0.25}$$

where $\bar{\sigma}_\varepsilon$ = standard derivation of vertical angle at the 40 meter level,

$\bar{u}$ = mean and speed, and

F = tree canopy density based on light intensity

measurements yielded the best fit to all available line source data. The longitudinal decay parameter from the Litton Systems study of -0.993 compares with a value of -0. for this work. In addition to modifications of simple Gaussian plume models (Tourin and Shen, 1969) (Allison, 1968), one may also appeal to a simple-minded one-dimensional model for canopy penetration, first suggested by Calder, (1961).

The below canopy concentrations resulting from an elevated continuous release line source can be estimated by,

$$C_{\substack{\text{below}\\ \text{canopy}}}(x) = \left(\frac{s}{u}\right)\exp\left(-\frac{s}{u}x\right)\int_0^x \exp\left(\frac{s}{u}y\right) C_{\substack{\text{above}\\ \text{canopy}}}(y)\,dy$$

where s = penetration coefficient and u = below canopy wind speed. The above canopy measurements have been fitted to the formula suggested by Bosanquet and Pearson (1936),

$$C_{\substack{\text{above}\\\text{canopy}}}(x) \doteq \frac{A}{x}\exp(-\,B/x),$$

and the predicted below canopy concentrations compared with experimental data in Figure (25). Obviously the Bosanquet formula is somewhat inadequate, however, it is apparent fair comparison is obtained for a model penetration coefficient of 0.75 $\sec^{-1}$. This is comparable to a prototype exchange rate of ~0.45 minutes^{-1} since the time scale for the model may be interpreted as 100 times less than in the field.

Calder also suggested a manner in which to check the validity of the mathematical model and estimate the parameter $H = s/u$. He noted that the model requires that

$$\frac{\int_0^\infty \exp(-px)\, C_{\substack{\text{below}\\\text{canopy}}}(x)\,dx}{\int_0^\infty \exp(-px)\, C_{\substack{\text{above}\\\text{canopy}}}(x)\,dx} = \frac{H}{p + H}$$

for different selected values of the transform parameter p. This equation was checked numerically for a range of p from 2 to 10, and the calculated parameter H varied from 1.92 to 1.14; whereas, the best first value from the figure appears to be 1.50.

Although the model for an instantaneous point source suggested by the MELPAR (1968) study incorporated vertical and lateral dispersion degrees of freedom their predictions were limited to below canopy release conditions. In addition, they incorporated an infinite mass sink at the canopy top, which was admitted to be over restrictive. Information concerning the vertical concentration profiles obtained in this study might be used to improve the MELPAR model, since no vertical measurements were available in the Jungle Canopy study.

Tourin and Shen also compared their measurements for elevated line source releases above a Wisconsin forest with Calder's model and another model developed from Lattau's hypothesis of vorticity transfer. These models generally did not agree with the observed data, as well as the regression equation; however, one can not tell whether this is a failure of the below canopy models utilized or the inadequacy of the Bosanquet-Pearson expression used to predict above canopy dosages.

5. CONCLUSIONS

It is apparent that the general character of flow in and above vegetative canopies may be satisfactorily simulated in the meteorological wind tunnel. In addition, these new data suggest that even the micro-structure transport phenomena behave in a manner similar to that of the prototype. Therefore, it is possible to conclude that:

1) The basic trends of the dynamic and kinematic behavior of a complex vegetative cover may be simulated by a simple porous geometry in a wind tunnel.

2) The initial fetch of the peg canopy affects tracer dispersion of a continuous point source in a unique manner: Vertical convective motions exhale the gases released at the beginning of the canopy, and subsequently, the canopy appears to re-inhale the products farther downstream.

3) The concentration profile above the canopy displays the features of a plume released over a flat plate but displaced by a height h.

4) The eddy diffusion coefficient varies linearly as $(z-d)$ above a vegetative cover and has a growth rate nearly proportional to $ku*$.

5) The eddy diffusion coefficient, K_z, within the artificial vegetative cover, appears to develop into three regions: Initially K_z grows exponentially, next it remains constant, and finally, K_z grows at a linear rate.

6) The experimental law for attenuation of boundary concentration was obtained as $x^{-4.8}$ for gas source releases

far from the canopy inception. (Rates of dispersion are somewhat larger near the edge of the vegetative cover.)

7) The lateral eddy diffusion coefficient, K_y, appears to be ~2 times larger than the vertical transport rate as on approximation. However, it is expected that $K_y \neq 0$ at ground level.

8) Considering the similarity of plume behavior when considered separately above and below the top of the canopy, it would appear that models directed to treat the physics of these two layers separately are justified.

BIBLIOGRAPHY

1. Allen, L. H., 1968: Turbulence and wind spectra within a Japanese Larch plantation. J. Applied Meteorology, 7, 73-78.

2. Allison, J. K., L. P. Herrington and J. P. Morton, 1968: Diffusion below and through a dense, high canopy. Paper PRC 68-3, Melpar, Inc., Arlington, Virginia. (Paper presented at Conference on Fire and Forest Meteorology of the American Meteorological Society and the Society of American Foresters, March 1968).

3. Baynton, H. W., 1963: The penetration and diffusion of a fine aersol in a tropical rain forest. Ph.D. Thesis, University of Michigan, Ann Arbor.

4. Bosanquet, C. H. and J. L. Pearson, 1936: The spread of smoke and gases from chimneys. Trans. Faraday Soc., 32: 1249-1263.

5. Brown, R. A., G. E. McVehil, R. L. Pearce, and R. W. Coakley, 1969: Characterization of Forest Vegetative Analogs, Technical Report Cornell Aeronautical Lab. CAL No. VT-2408-P-1, 20 March.

6. Burgy, R. H., 1961: Aerodynamics drag on tall vegetation: Studies of three-dimensional structure of the planetary boundary layer. Annual Dept., Dept. of Meteorology, University of Wisconsin, pp 37-44.

7. Calder, K., 1961: A simple mathematical model for the penetration of forest canopy by aerosols. U.S. Army Chemical Corps, Biological Laboratory Technical Study 37, Fort Detrick, AD 262228.

8. Cooper, R. W., 1965: Wind movement in pine stands. Georgia Forest Res. Paper No. 33, Georgia Forest Res. Council.

9. Denmead, O. T., 1964: Evaporation sources and apparent diffusivities in a forest canopy. J. Applied Meteorology 3, 383-389.

10. Fons, W. L., 1940: Influence of forest cover on wind velocity. J. Forestry, 38, 481-486.

11. Flemming, G., 1967: Concerning the affect of terrain configuration on smoke dispersal. Atmospheric Environment, Vol. 1, pp. 239-252.

12. Geiger, R., 1950: The climate near the ground. Harvard University Press, Cambridge.

13. Hirata, T., 1953: Fundamental studies on the formation of cutting series on the center pressure, the drag coefficient of a tree and one effect of shelter belts. Bull. Tokyo University Forestry, No. 45, 61-87.

14. Hsi, G. and J. H. Nath, 1968: A laboratory study on the drag force distribution within model forest canopies in turbulent shear flow. Fluid Dynamics and Diffusion Laboratory, Report No. CER67-68GH-JHN50.

15. Huston, J. S., 1964: Observations of the micrometeorology and intensity of turbulence within a deciduous forest. Chemical Development Laboratory, Memo 5-6, (AD447911).

16. Iizuka, H., 1952: On the width of a windbreak. Bull. Forestry Exp. Sta., Meguro, Tokyo, 56, 1-218.

17. Iizuka, H., 1956: On the width of windbreak. Proc. Intern. Union of Forest Res. Organ., 12th Congress, Oxford, Section II, IUFRO, 1-4.

18. Inoue, E., 1963: On the turbulent structure of airflow within crop canopies. Journal of Meteorological Society of Japan, Series II, 41, #6.

19. Kung, E., 1961: Derivation of z_o from wind profile data above tall vegetation. Annual Report DA-36-039-SC-80282, U. S. Army Electronics Command, Ft. Huachuca, 27-36.

20. Lai, W. 1955: Aerodynamic drag of several broadleaf tree species. Internal Tech. Report, AFSWP-863, U. S. Dept. Agriculture, Forest Service.

21. Lemon, E. R., (ed), 1962: The energy budget at the earth's surface. Part II, Production Research Report No. 2, Agricultural Research Service, U. S. Dept. of Agriculture, p. 49.

22. Malhotra, R. C. and J. E. Cermak, 1964: Mass diffusion in neutral and unstably stratified boundary-layer flows. International Journal of Heat and Mass Transfer, 7, 169-186.

23. Malina, F. V., 1941: Recent developments in the dynamics of wind-erosion, Trans. Amer. Geophys. Union, p. 279.

24. MELPAR, Inc., 1968: Diffusion under a jungle canopy. Final Report, Vol. 1, Contract DA-42-007-AMC-33CR U.S. Army Dugway Proving Ground, February, 187 pages.

25. Meroney, R. N., 1968: Characteristics of wind and turbulence in and above model forests. Journal of Applied Meteorology, 7, #5, 780-788.

26. Meroney, R. N. and J. E. Cermak, 1967: Characteristics of diffusion within model canopies. Paper presented at Symposium on the Theory and Measurement of Atmospheric Turbulence and Diffusion in the Planetary Boundary Layer, Albuquerque.

27. Peaceman, D. W. and H. H. Rachford, 1955: The numerical solution of parabolic and elliptic differential equations. Journal Soc. Indust. Applied Math, Vol. 3, No. 1, pp. 28-41.

28. Penman, H. L. and I. F. Long, 1960: Weather and wheat. Quarterly Journal of Royal Meteorological Society, 86, 16-50.

29. Plate, E. J. and J. E. Cermak, 1963: Micro-meteorological wind tunnel facility: Description and characteristics. Fluid Dynamics and Diffusion Laboratory, Tech. Report CER63EJP-JEC9, Colorado State University.

30. Plate, E. J. and A. A. Quarishi, 1965: Making of velocity distributions inside and above tall crops. Journal of Applied Meteorology, 4, #3, 400-408.

31. Poppendiek, H. F., 1949: Investigation of velocity and temperature profiles in air layers within and above trees and brush, Tech. Report Contract N6-ONT-275, Task Order VI, NR-082-036, Dept. of Engineering, University of California, Los Angeles.

32. Rayner, W. G., 1962: Wind resistance of conifers. National Physical Laboratory, Aero. Dept., 1008.

33. Raynor, G. S., 1969: Forest micro meteorology studies at Brookhaven National Laboratories. Fourth Annual George H. Hudson Symposium, State University College of Arts and Science, Plattsburgh, New York, March 26-28, 1969.

34. Raynor, G. S., 1967: Effects of a forest on particulate dispersion. USAEC Meteorological Information Meeting, Chalk River, Canada.

35. Reifsnyder, W. E., 1955: Wind profiles in a small isolated forest stand. Forest Sci., 1, No. 4, 289-297.

36. Reinke, L. H., 1933: Perfecting a stand-density index for even aged forests. J. Agr. Res., 46, 622-628.

37. Robinson, S. M., 1961: A method for machine computation of wind profile parameters. and, Studies of the three-dimensional structure of the planetary boundary layer. Annual Report DA-36-039-SC-80282, U. S. Army Electronics Command, Ft. Huachuca, 63-70.

38. Sadeh, W. Z., J. E. Cermak, and T. Kawatani, 1969: Flow field within and above a forest canopy. Technical Report CER69-70WZS-JEC-TK6, Fluid Dynamics and Diffusion Laboratory, Colorado State Univ., July.

39. Saito, T., 1964: On the wind profiles in plant communities. Bulletin of the National Institute of Agricultural Science, Japan, Series A, #11.

40. Sauer, F. M., W. L. Fons, and K. Arnold, 1951: Experimental investigation of aerodynamic drag in tree crowns exposed to steady wind-conifers. Dept. Div. Forest Fire Res., U.S. Dept. Agriculture, Forest Service.

41. Shinn, J.,1969: Analysis of wind data from a South Carolina coastal forest. U.S. Army Electronics Command, Research and Development Technical Department, ECOM-6036.

42. Shinn, J., 1969: Private Communication, ASRTA, Fort Huachuca, Arizona (1969).

43. Tiren, Lars, 1927: Einige interschungen ober die schaftform. Meddel. Stattens Skogsforsoksanstalt, Hafte 24, No. 4, 81-152.

44. Tourin, M. H. and W. C. Shen, 1966: Deciduous forest diffusion study. Final Report to U.S. Army, Dugway Proving Grounds, Contract DA42-007-AMC-48(R).

45. Uchijima, Z. and J. L. Wright, 1964: An experimental study of air flow in a corn plan-air layer. Bulletin of the National Institute of Agricultural Sciences, Japan, Series A, #11.

46. Walske, D. E. and A. I. Fraser, 1963: Wind tunnel tests on a model forest. National Physical Laboratory, Aero. Report, 1078.

47. Woodruff, N. P., and A. W. Zingg, 1952: Wind tunnel studies of fundamental problems related to windbreaks. U.S. Dept. Agriculture, Soil Conservation Service, Report SCS-TP-112.

48. Wright, J. L. and E. R. Lemon, 1961: Estimation of turbulent exchange within a corn crop canopy at Ellis Hollow (Ithaca, New York), Internal Report 62-7, New York State College of Agriculture, Cornell University, 1962.

49. Yano, Motoaki, 1966: Turbulent diffusion in a simulated vegetative cover. Fluid Dynamics and Diffusion Laboratory Tech. Report CER66MY25, Colorado State University.

Concentration Profiles of Diffusion in the Plastic Tree Canopy

$\frac{\chi V_\infty}{Q} = 38.7\ \chi(cm^{-2})$ $X_s = 0^m$ $Q = 15.5$ cc/sec

$Z_s = 0^{cm}$

Source: Helium
Unit: ppm

X(m) / Z(cm)	1/4	1/2	3/4	1	1 1/2	2	2 1/2
0	7077	2101	1245	968	499	63	56
1	4390	1908	1259	913	512	65	55
2	2197	1563	1272	982	512	63	55
3	210	1410	1259	900	526	66	58
4	193	775	1134	900	512	78	58
5	96	457	1093	850	512	73	61
6	26	383	1051	830	499	73	60
8	9.7	203	1065	803	443	81	61
10	------	133	1065	816	443	81	63
12	------	89	1038	830	499	86	65
14	------	69	872	775	499	90	68
16	------	----	526	656	499	98	73
18	------	----	333	540	457	103	71
20	------	----	153	415	443	103	75
22	------	----	89	259	346	103	73
24	------	----	54	143	291	103	70
26	------	----	----	83	236	103	73
28	------	----	----	---	194	102	70
30	------	----	----	---	153	95	70
34	------	----	----	---	97	88	68
40	------	----	----	---	44	71	68
46	------	----	----	---	---	51	55
50	------	----	----	---	---	41	51

Table 1

Concentration Profiles of Diffusion in the Plastic Tree Canopy

$\frac{\chi V_\infty}{Q} = 38.7\ \chi (cm^{-2})$ $X_s = 0^m$ $Q = 15.5$ cc/sec

Source: Helium $Z_s = 10^{cm}$

Unit: ppm

X(m)	1/4	1/2	3/4	1	1 1/2	2	2 1/2
Z(m)							
0	----	---	---	-----	--	7	26
1	----	---	---	-----	--	7	27
2	----	7	---	-----	--	11	29
3	4	6	2	-----	--	13	27
4	27	10	3	-----	--	13	26
5	55	12	5	-----	--	14	25
6	145	23	8	2.5	--	20	27
8	283	28	9	2.5	--	20	27
10	583	51	7	2.5	--	25	26
12	3163	51	11	2.5	2	26	27
14	4063	79	13	13	18	30	30
16	3713	151	30	36	27	32	32.5
18	1543	419	64	64	36	31	36
20	643	909	119	74	36	36	36
22	263	909	229	97	50	46	36
24	27	559	319	128	59	46	36
26	9	327	344	154	59	46	36
30	5	59	242	174	64	46	36
34	----	---	64	136	74	54	34
40	----	---	---	36	54	46	32
46	----	---	---	-----	32	36	27

Table 2

Concentration Profiles of Diffusion in the Plastic Tree Canopy

$\frac{\chi V_\infty}{Q} = 38.7\ \chi(cm^{-2})$ $X_s = 6^m$ $Q = 15.5$ cc/sec

$Z_s = 0^{cm}$

Source: Helium
Unit: ppm

	(4cmE)	(8cmE)	(12cmE)	(10cmE)	(3cmW)	(6cmW)	(8cmW)
X(m)	1/4	1/2	3/4	1	1 1/2	2	2 1/2
Z(cm)							
0	2777	1517	750	380	90	17	8
1	2497	1377	430	408	122	16	8
2	2497	1227	485	355	85	17	7
3	3357	1087	355	300	84	24	8
4	3067	947	355	355	106	19	7
5	3067	947	330	250	84	15	7
6	3357	1087	380	223	87	24	8
8	2227	947	300	170	71	15	9
10	2227	807	250	105	59	20	9
12	1517	662	223	78	47	19	11
14	1087	523	144	78	47	19	12
16	662	324	118	60	45	17	12
18	297	240	105	65	40	21	14
20	240	210	78	65	40	21	15
22	100	140	65	65	34	20	15
24	100	127	78	65	31	19	14
26	41	84	65	39	34	18	14
30	13	54	52	39	24	19	14
34	----	----	---	---	17	14	12
40	----	----	---	---	13	12	11
46	----	----	---	---	10	11	8

Table 3

Concentration Profiles of Diffusion in the Plastic Tree Canopy

$\frac{\chi V_\infty}{Q} = 38.7\ \chi(\mathrm{cm}^{-2})$ $X_s = 6^m$ $Q = 15.5$ cc/sec

$Z_s = 10^{cm}$

Source: Helium
Unit: ppm

X(m)	1/4	1/2	3/4	1	1 1/2	2	2 1/2
Z(cm)							
0	304	139	78	68	64	57	49
1	352	142	96	83	68	56	51
2	364	130	102	85	68	59	51
4	408	139	99	83	71	58	52
6	427	149	105	89	69	57	54
8	408	150	125	81	76	61	56
10	419	160	128	83	82	63	54
12	507	171	123	94	78	68	54
14	530	186	114	101	78	67	59
16	578	200	115	106	85	67	61
18	471	198	139	114	89	67	62
20	451	196	133	104	89	70	59
22	455	175	127	105	89	68	62
24	412	167	131	103	85	68	62
26	324	164	127	103	85	68	59
30	209	142	110	105	79	70	59
34	89	98	898	80	76	64	57
38	54	73	72	76	68	61	59
42	32	55	66	66	65	59	52
46	---	---	49	58	60	52	49
50	---	---	39	54	54	49	48
55	---	---	---	---	--	47	45

Table 4

Concentration Profiles of Diffusion in the Plastic Tree Canopy

$\frac{\chi V_\infty}{Q} = 2.56\ \chi(cm^{-2})$ $X_s = 6^m$ $Q = 235\ \mu\mu$ ci/sec

$Z_s = 10^{cm}$

Source: Kr-85
Unit: $\mu\mu$ ci/cc

X(m) / Z(cm)	1/4	1/2	3/4	1	1 1/2	2	2 1/2	3
0	7000	2000	1150	560	339	292	266	206
2	10120	2121	1243	561	400	261	360	202
4	12680	2299	1245	688	387	317	266	211
6	21410	2096	1201	598	401	285	319	166
8	25060	2759	1279	629	427	291	335	184
10	33300	2336	914	556	326	287	194	163
12	154100	2762	1300	668	473	282	281	252
14	38760	3283	1154	681	464	331	258	215
16	16990	2777	1219	865	579	372	240	184
18	10240	2672	1340	787	477	363	288	170
20	6330	2522	1207	782	477	389	228	151
22	3456	2483	1223	700	449	281	271	213
24	1640	1895	775	586	320	293	144	152
26	1120	1697	984	687	403	294	249	165
28	435	1446	796	646	393	309	302	206
30	350	1060	744	589	362	257	255	220
32	264	883	662	489	321	261	240	163
34	106	489	558	426	362	213	233	170
36	44	380	294	354	300	240	210	166
38	------	261	227	240	205	129	204	126
40	------	232	309	250	235	158	199	102
42	------	54	153	151	165	149	99	87
44	------	42	104	123	148	156	142	58
46	------	----	54	106	118	132	92	66
48	------	----	----	75	120	111	128	61
50	------	----	----	---	---	141	89	48

Table 5

Concentration Profiles of Diffusion in the Plastic Tree Canopy

$\frac{\chi V_\infty}{Q} = 2.56\ \chi(cm^{-2})$ $X_s = 6^m$ Q = 235 μμ ci/sec

Source: Kr-85 $Z_s = 18^{cm}$

Unit: μμ ci/cc

X(m) / Z(cm)	1/4	1/2	3/4	1	1 1/2	2	2 1/2	3
0	1705	2250	1500	600	316	239	203	80
2	1557	2461	1637	678	354	341	260	205
4	1944	2684	1580	763	408	283	259	130
6	3152	2772	1487	750	421	370	201	122
8	4739	3140	1509	809	363	276	280	202
10	4534	2496	1088	556	261	183	152	121
12	6889	2873	1458	805	395	284	212	134
14	6291	2984	1868	980	413	309	263	144
16	6809	2661	1539	971	467	327	236	202
18	5768	2575	1448	974	538	276	247	194
20	4870	2228	1427	920	523	326	307	177
22	2978	1717	1385	906	440	286	246	171
24	1697	1165	788	562	459	211	178	819
26	1676	1415	1008	795	449	254	217	188
28	650	936	813	661	381	268	232	165
30	367	644	679	543	383	344	212	137
32	204	474	469	489	247	235	206	175
34	130	329	355	495	268	228	180	120
36	81	384	387	322	281	145	147	110
38	32	213	242	154	168	144	803	47
40	26	141	229	235	149	134	139	114
42	----	58	156	167	180	125	146	82
44	----	40	38	161	177	102	149	117
46	----	----	----	111	130	94	123	101
48	----	----	----	80	125	96	97	92
50	----	----	----	50	109	60	---	65

Table 6

Concentration Profiles of Diffusion in the Plastic Tree Canopy

$\frac{\chi V_\infty}{Q} = 2.56\ \chi\,(cm^{-2})$ $X_s = 6^m$ $Q = 235\ \mu\mu$ ci/sec

$Z_s = 27^{cm}$

Source: Kr-85
Unit: $\mu\mu$ ci/cc

X(m) / Z(cm)	1/4	1/2	3/4	1	1 1/2	2	2 1/2	3
0	40	313	914	711	410	166	170	150
2	28	403	994	845	460	204	249	141
4	75	470	1091	717	411	213	180	218
6	109	485	1024	862	394	216	185	235
8	134	610	1064	736	421	274	234	233
10	96	587	1064	643	315	196	102	142
12	126	999	1007	656	440	262	198	244
14	184	713	901	693	115	347	232	225
16	262	937	830	660	435	386	229	221
18	605	845	879	704	392	268	199	216
20	1349	1170	927	652	396	300	273	211
22	2886	1590	950	596	481	329	197	263
24	2513	1032	767	426	335	166	133	141
26	4815	1536	859	654	418	254	240	185
28	3239	1149	691	537	413	278	208	199
30	2749	1193	671	454	322	271	175	131
32	1649	1216	622	428	228	237	137	139
34	909	828	597	387	244	185	192	156
36	569	569	501	422	229	241	155	181
38	233	352	270	316	138	145	79	91
40	250	320	388	313	161	198	137	124
42	110	77	170	182	117	182	118	149
44	----	97	152	153	136	115	138	150
46	----	48	42	123	111	125	130	109
48	----	20	49	135	70	158	118	85
50	----	----	----	72	---	69	127	91

Table 7

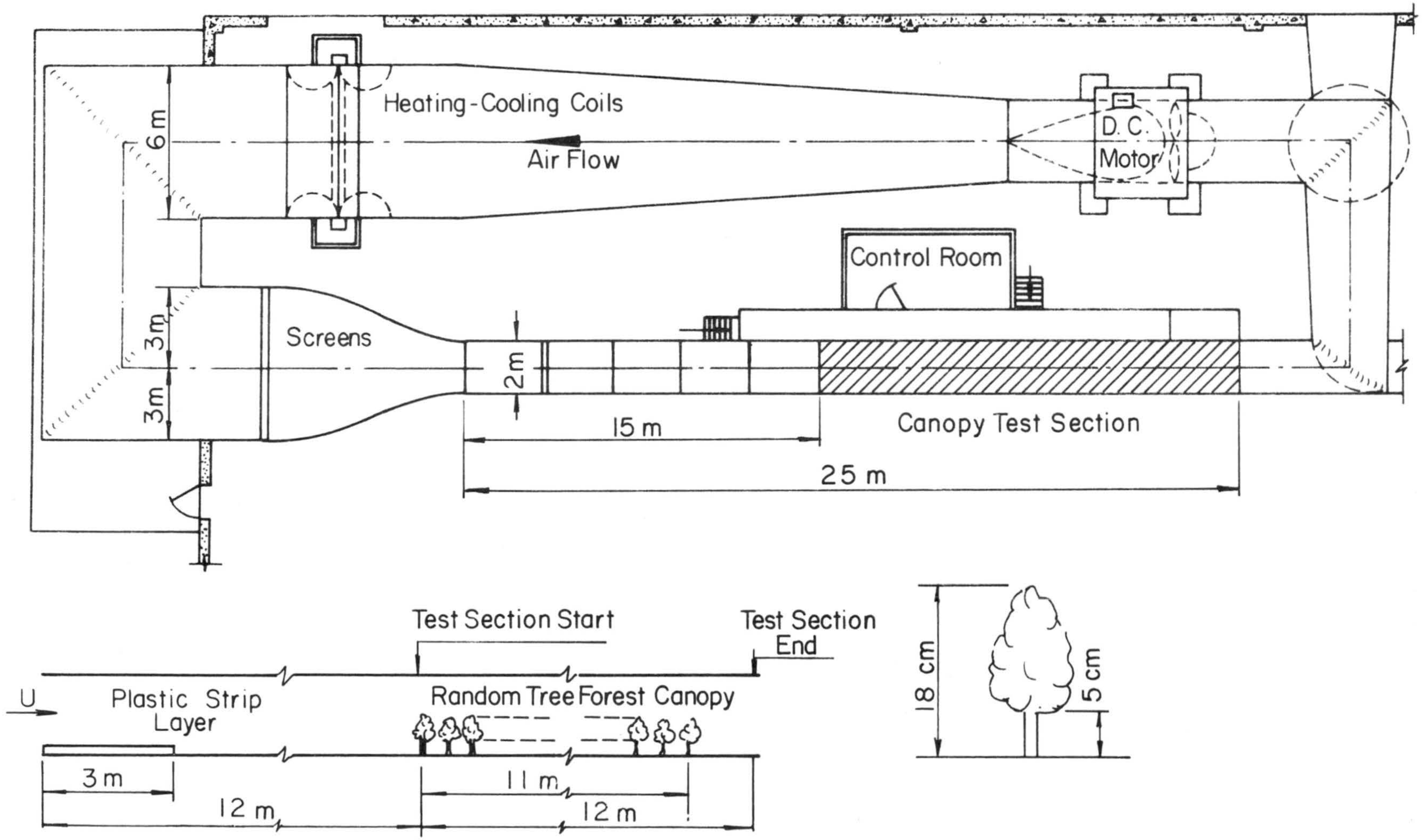

Figure 1. Wind tunnel arrangement.

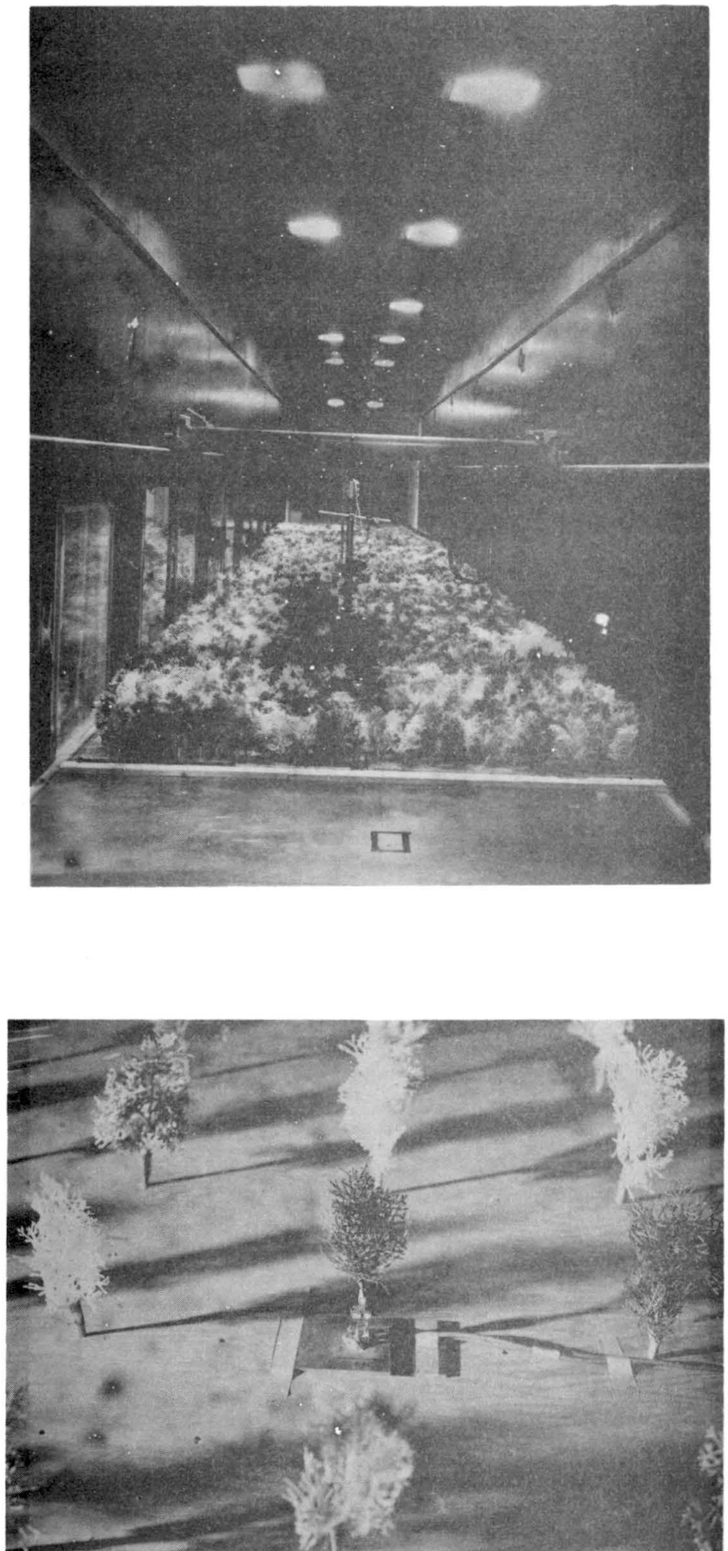

Figure 2. Model plastic forest.

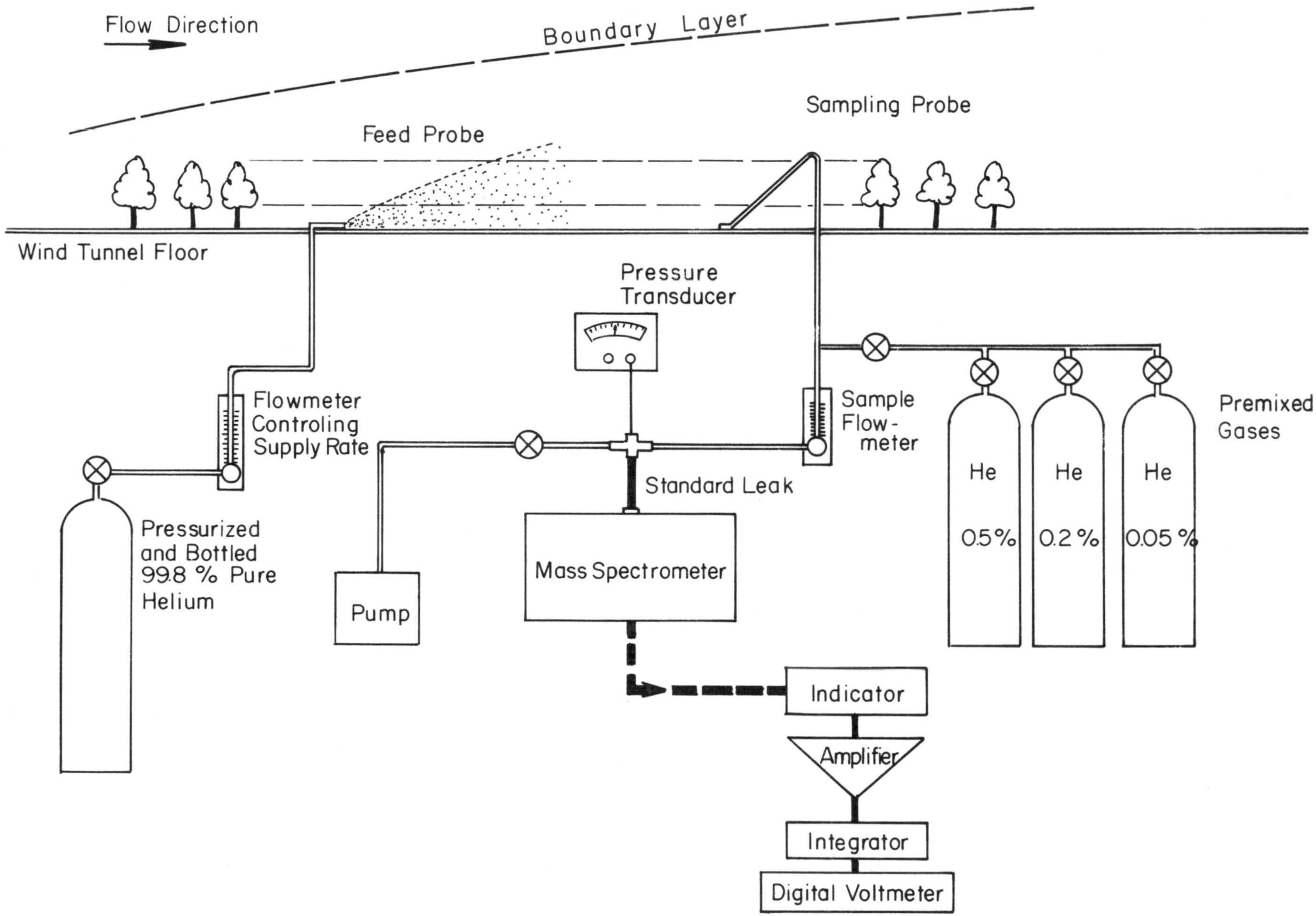

Figure 3. Helium detection system.

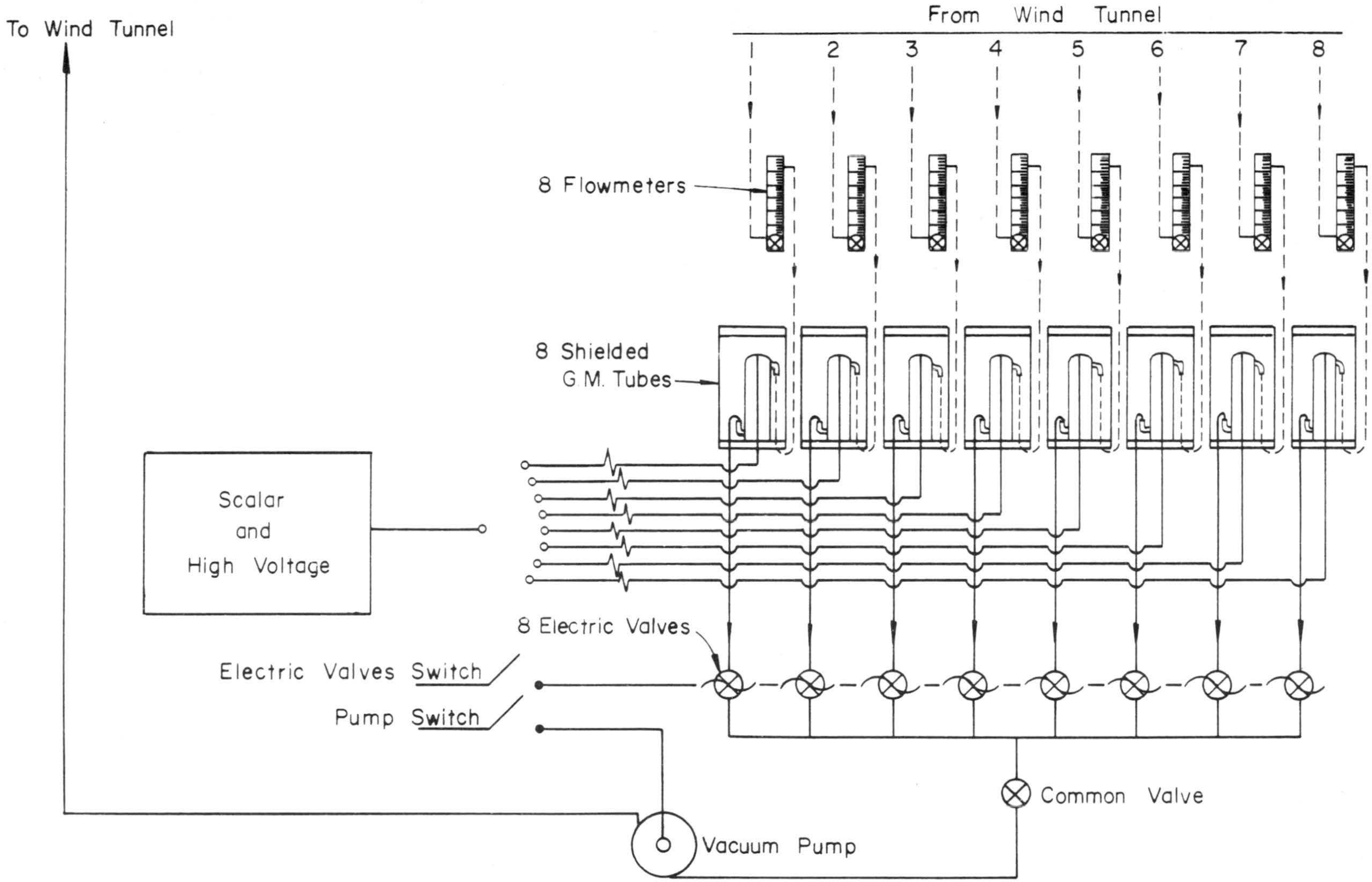

Figure 4a. Krypton-85 detection system - source.

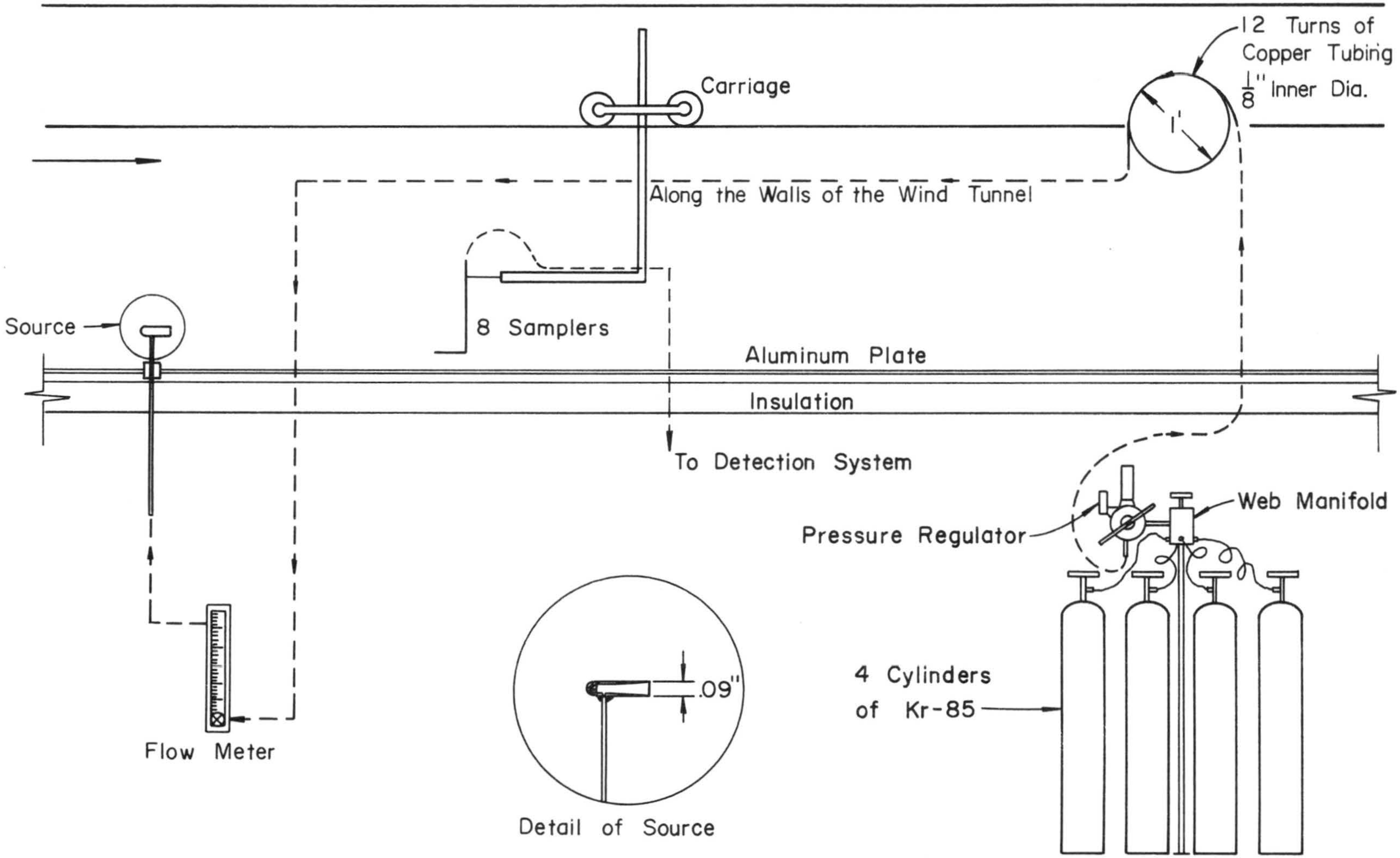

Figure 4b. Krypton-85 detection system - detector.

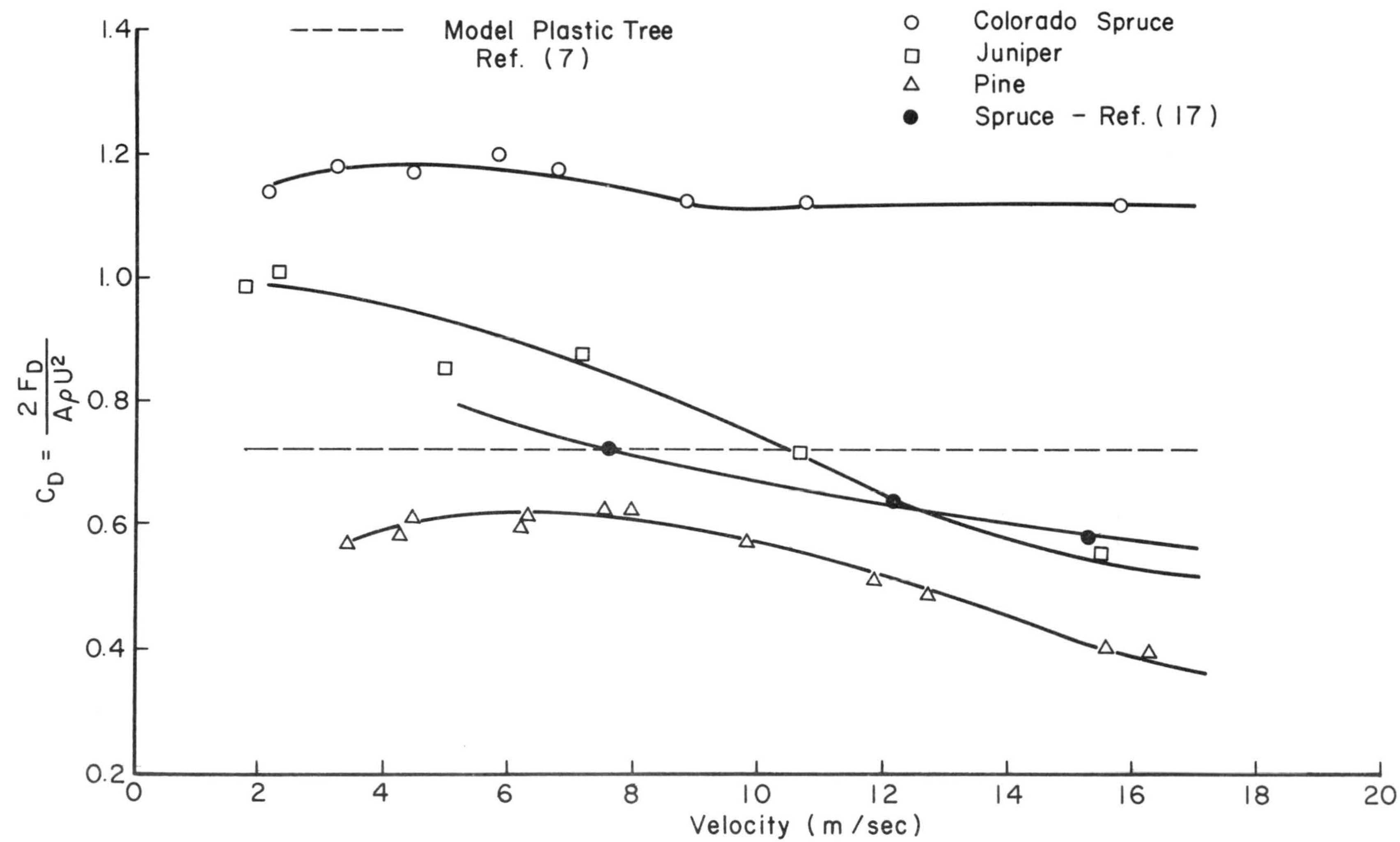

Figure 5. Drag coefficient of live and model trees.

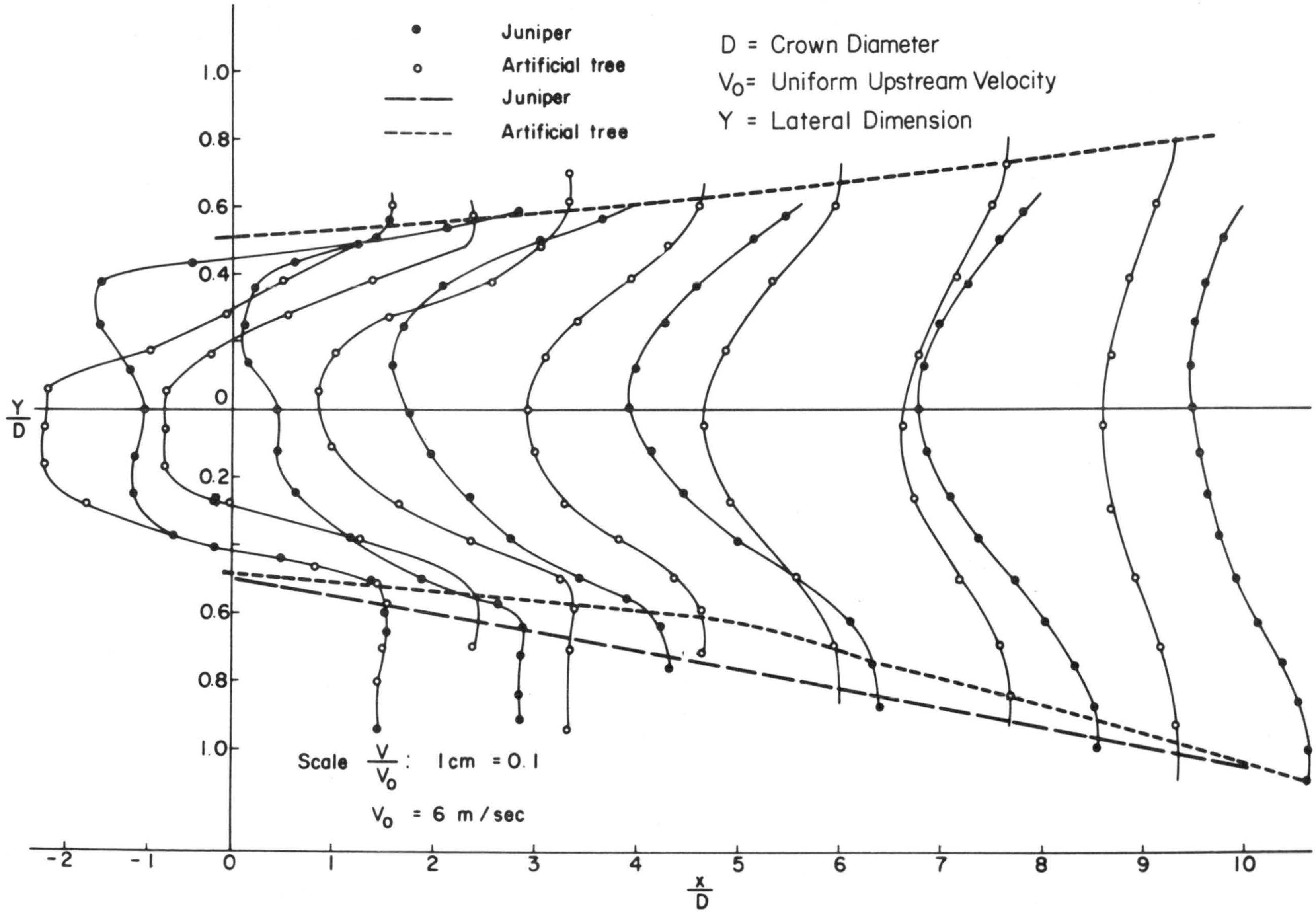

Figure 6. Wake characteristics of live and model trees.

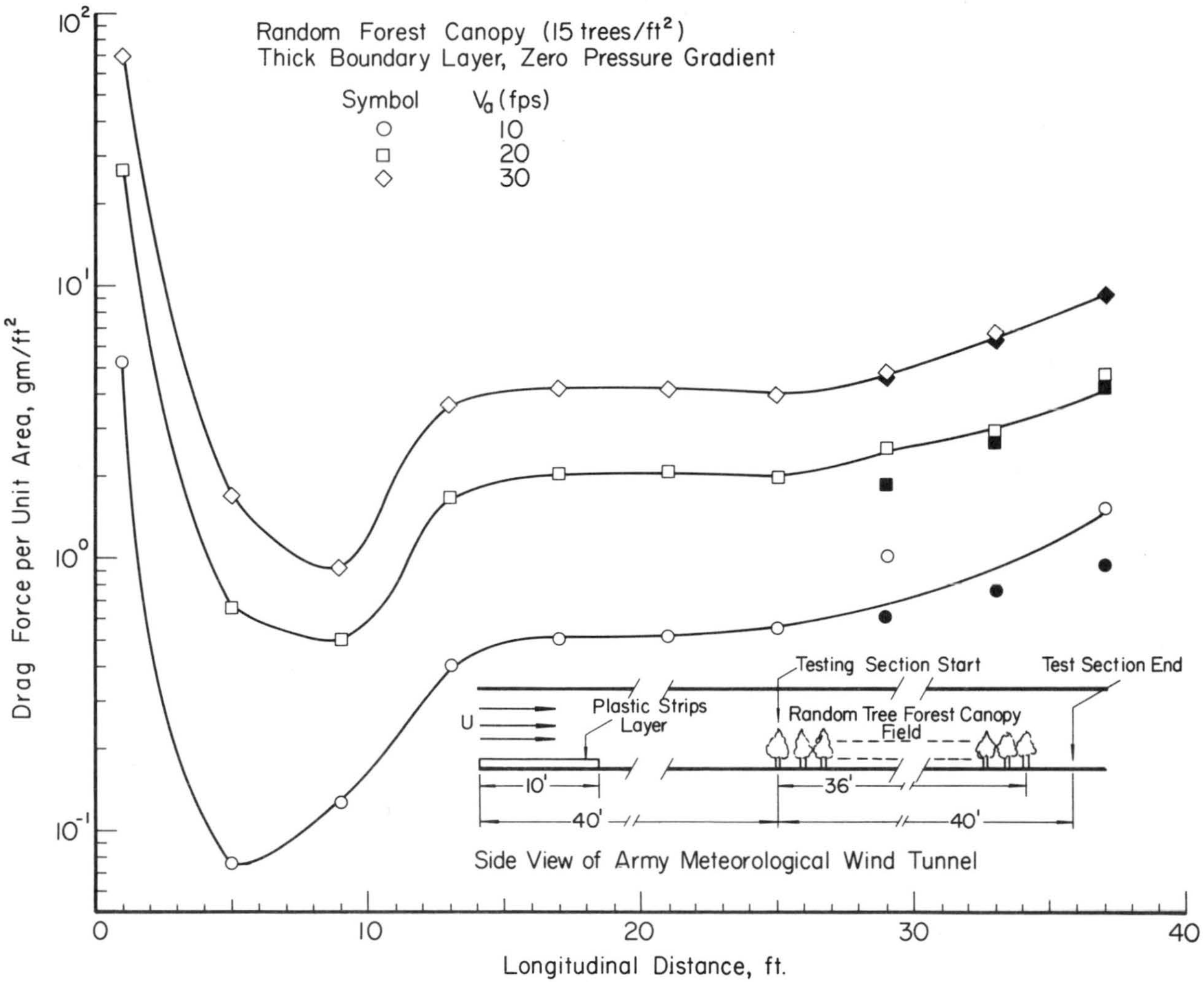

Figure 7. Shear plate drag for model forest canopy.

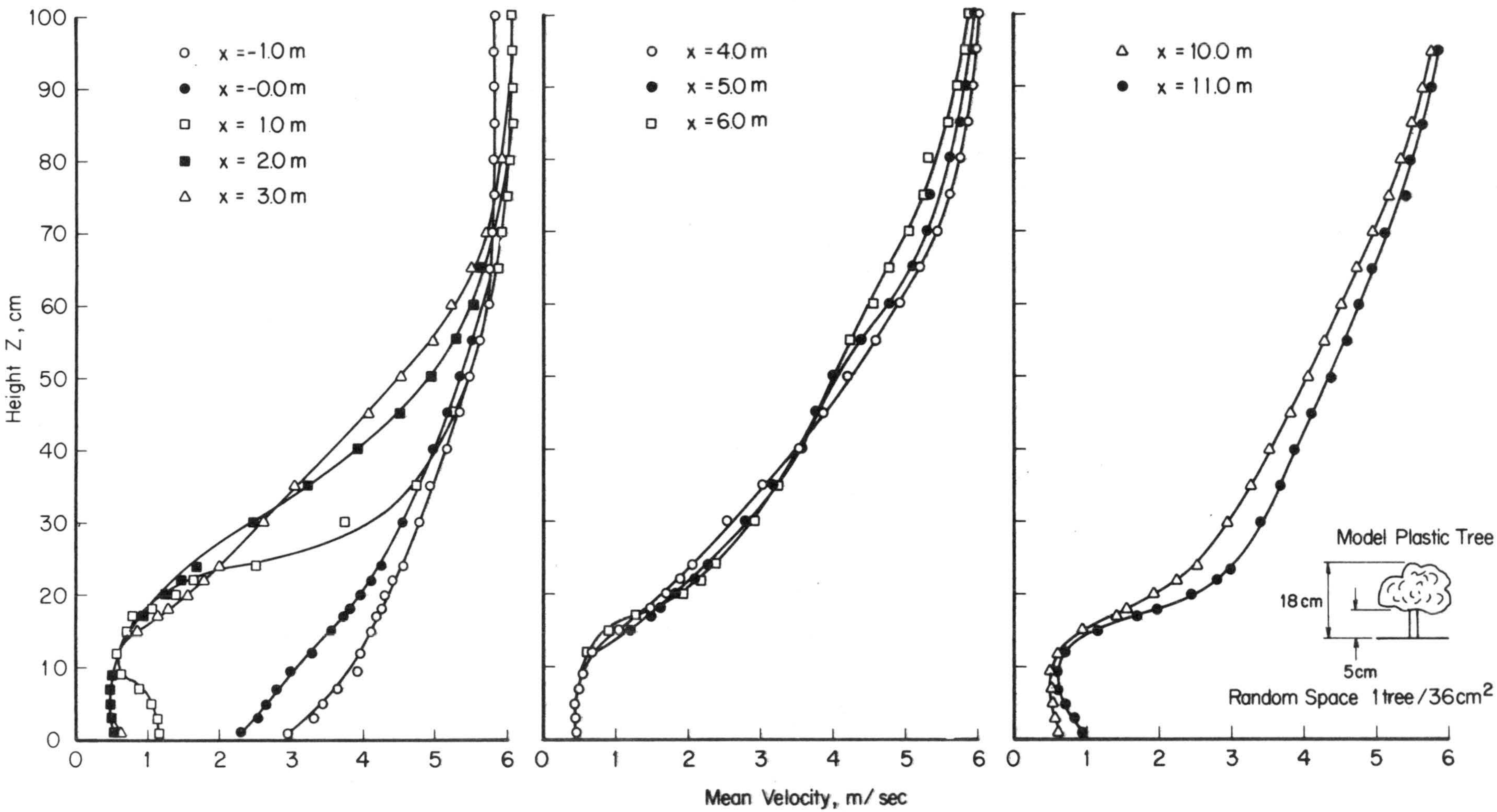

Figure 8. Velocity profiles.

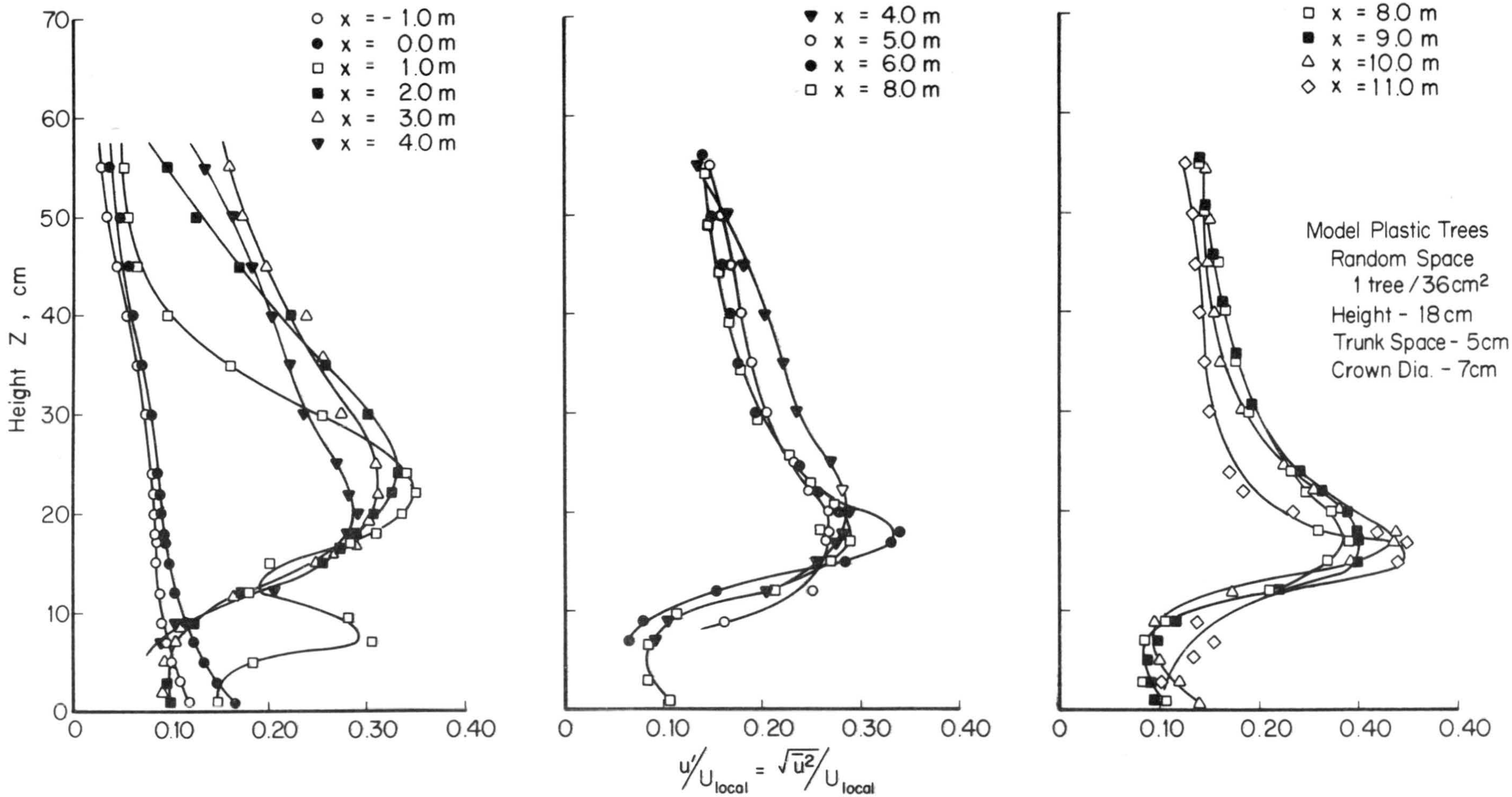

Figure 9. Turbulence intensities.

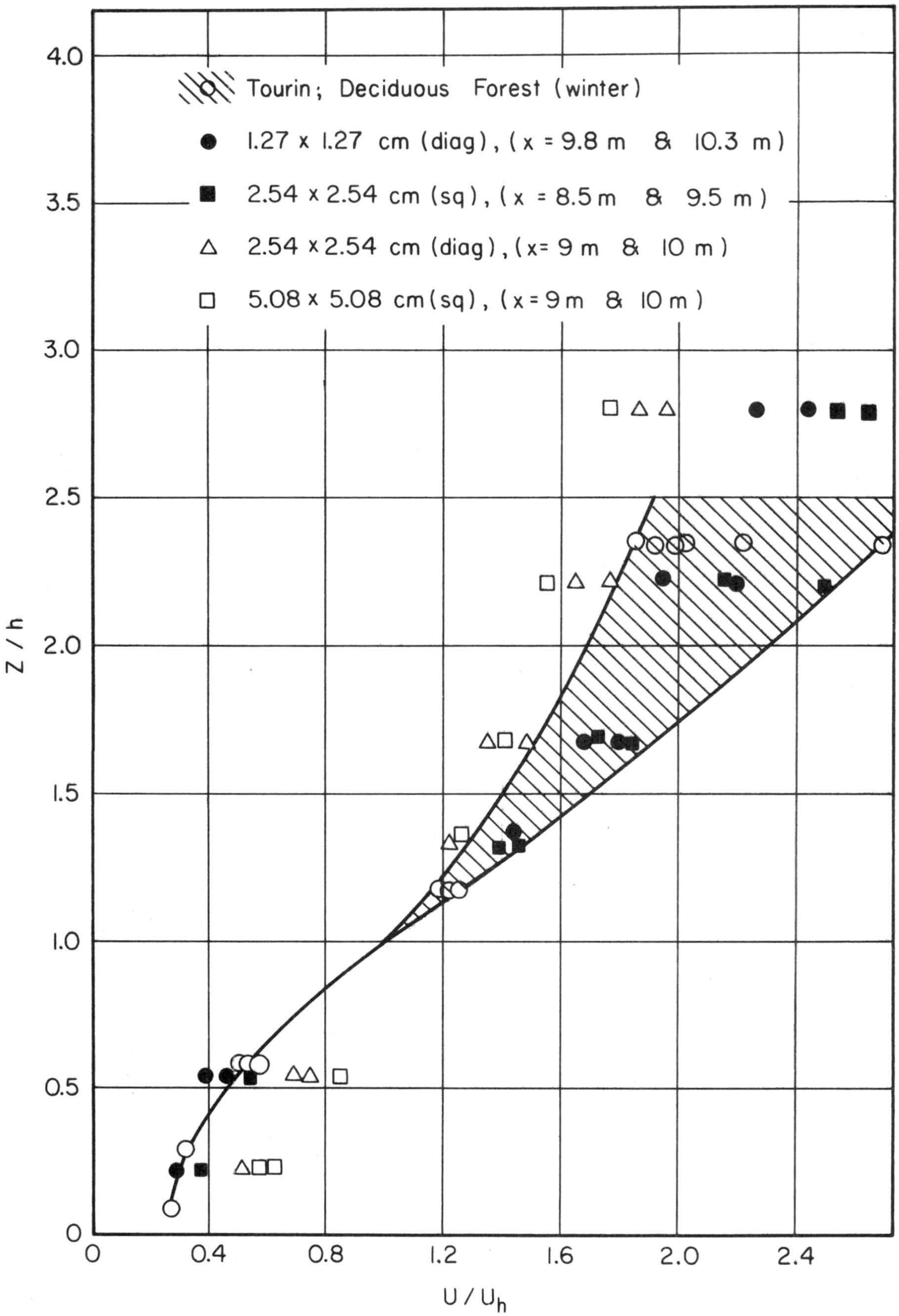

Figure 10. Comparisons with winter forests.

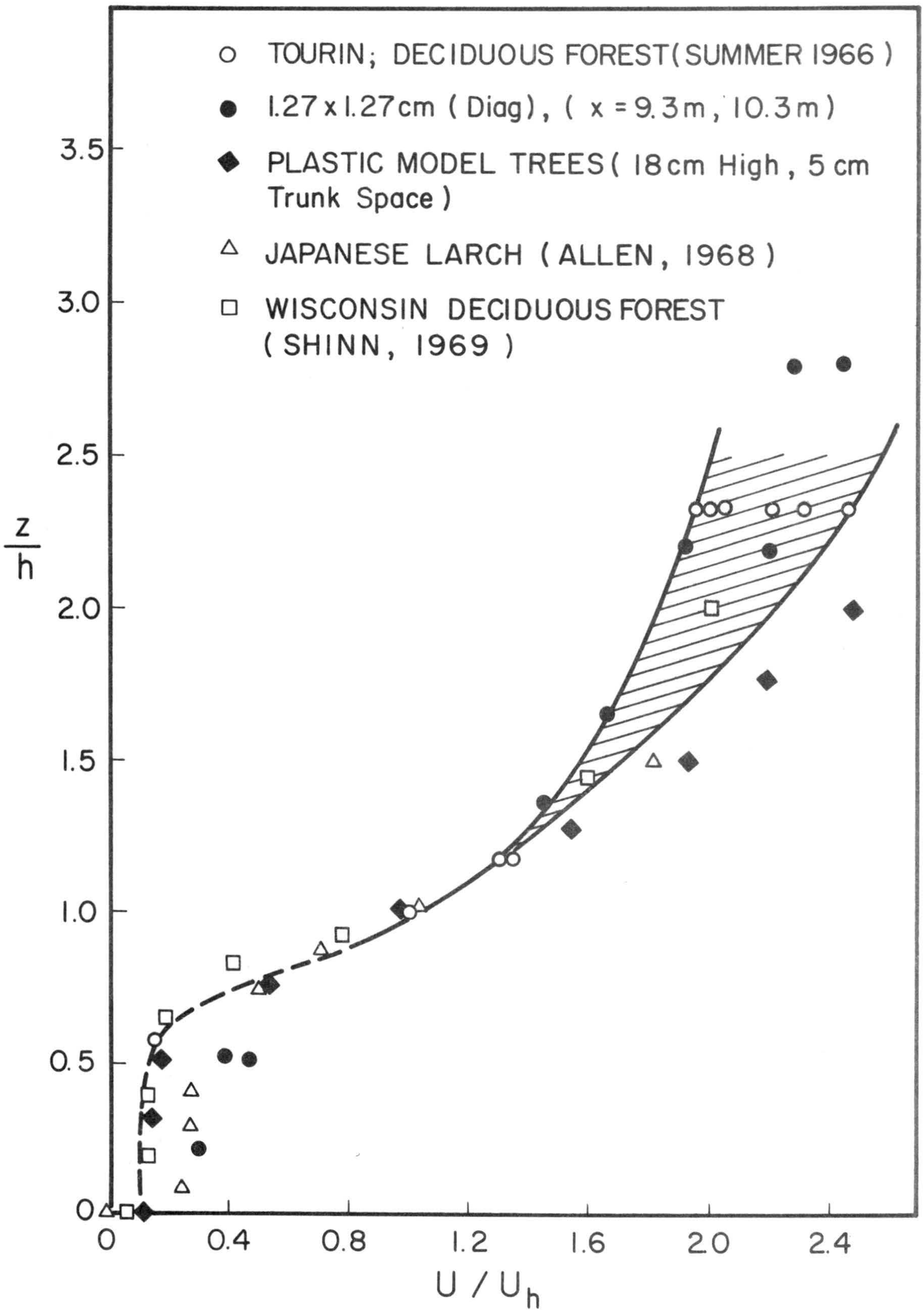

Figure 11. Comparisons with summer forests.

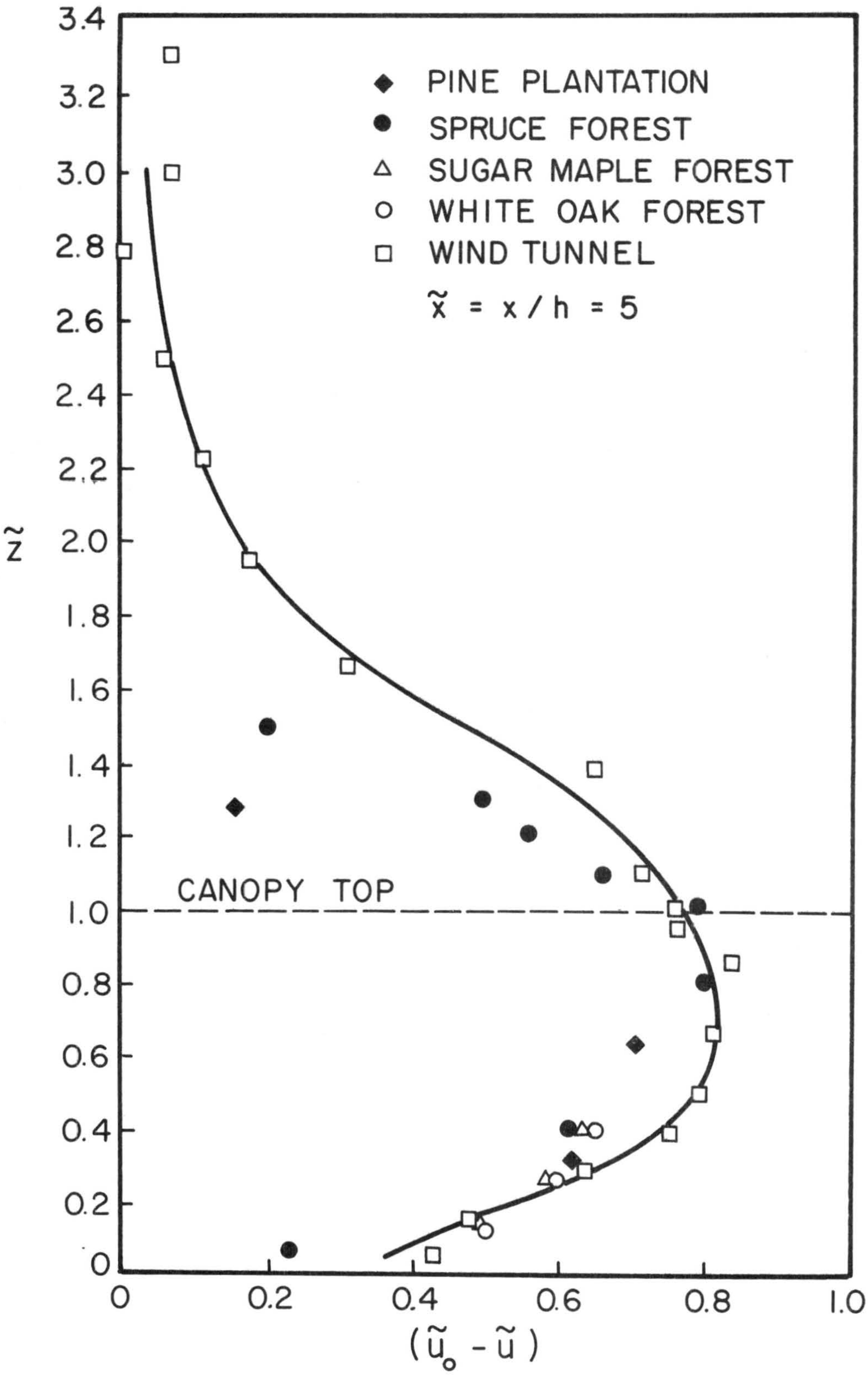

Figure 12. Velocity defect comparison.

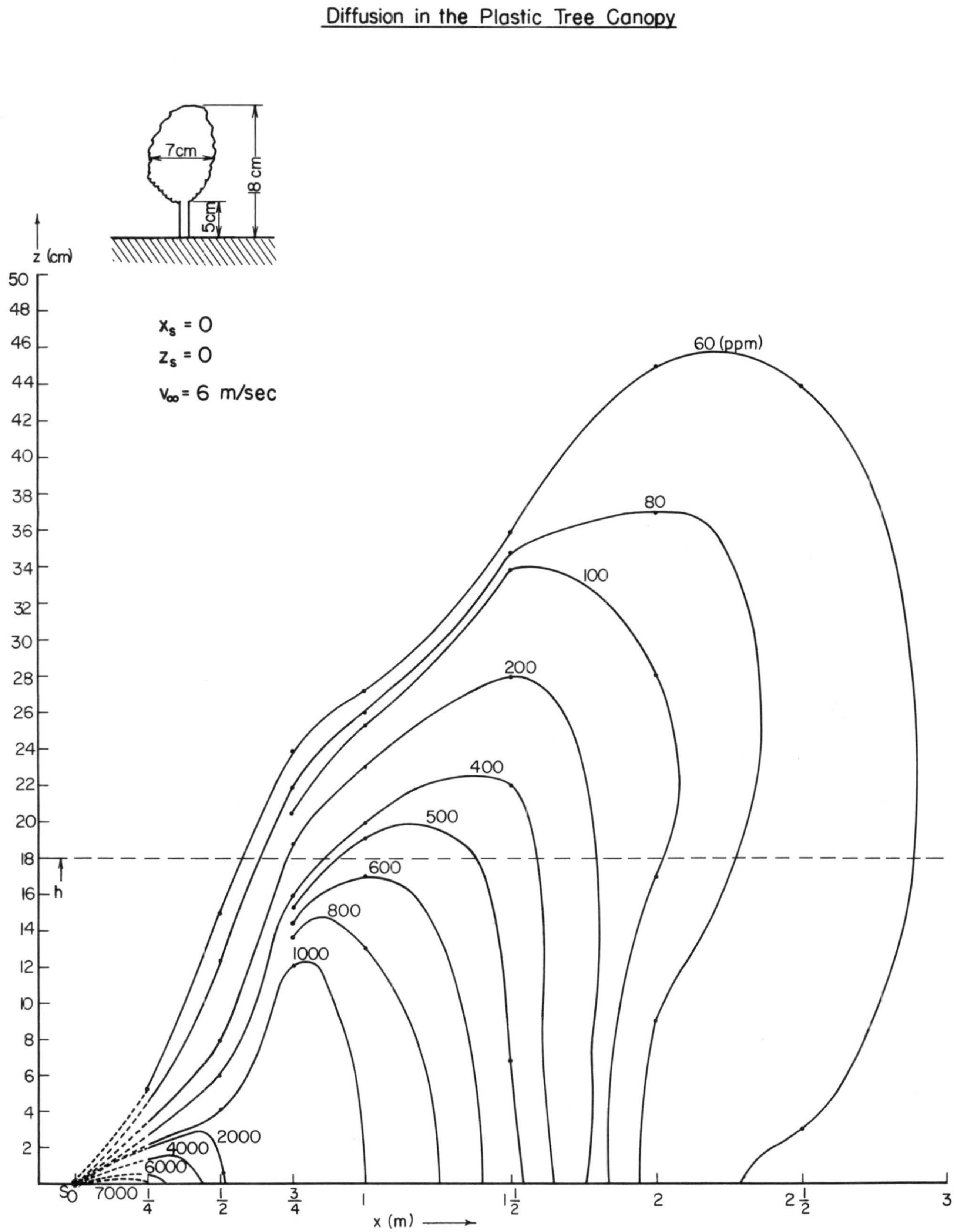

7

Figure 13. Diffusion - Isoconcentration profiles.
zs = 0.0 cm
xs = 0.0 m

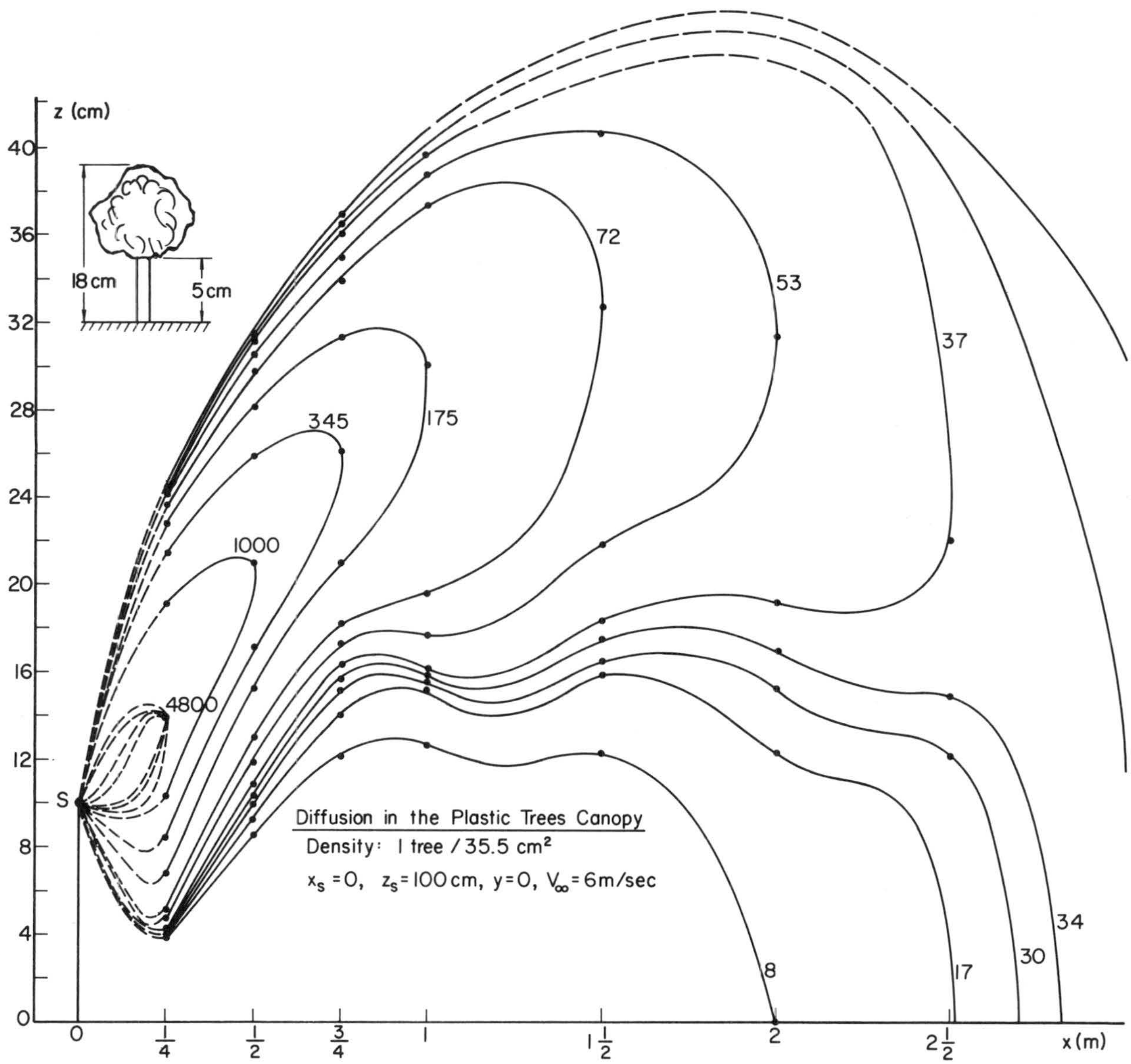

Figure 14. Diffusion - Isoconcentration profiles.
zs = 10.0 cm
xs = 0.0 m

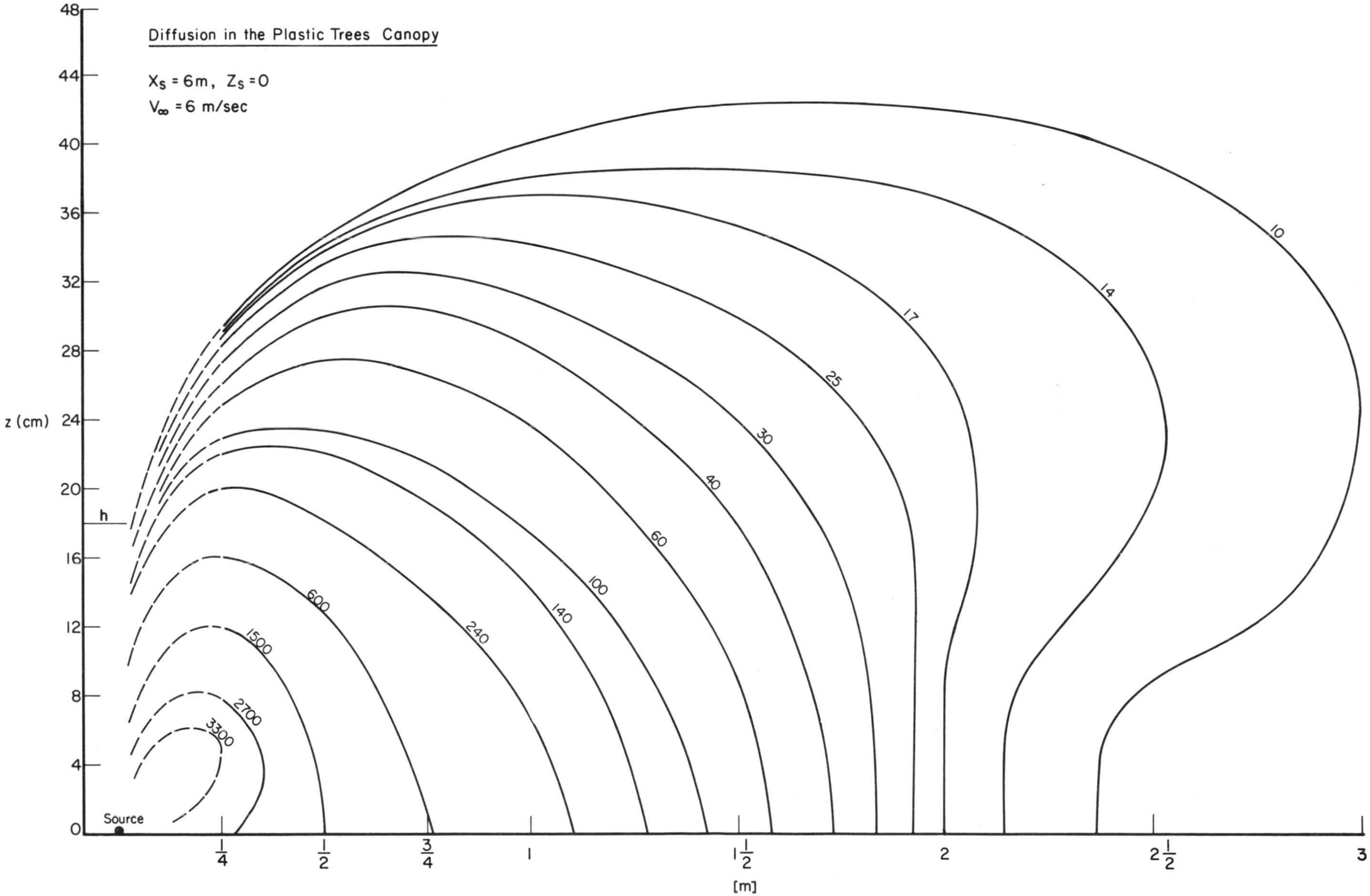

Figure 15. Diffusion - Isoconcentration profiles.
zs = 0.0 cm
xs = 6.0 m

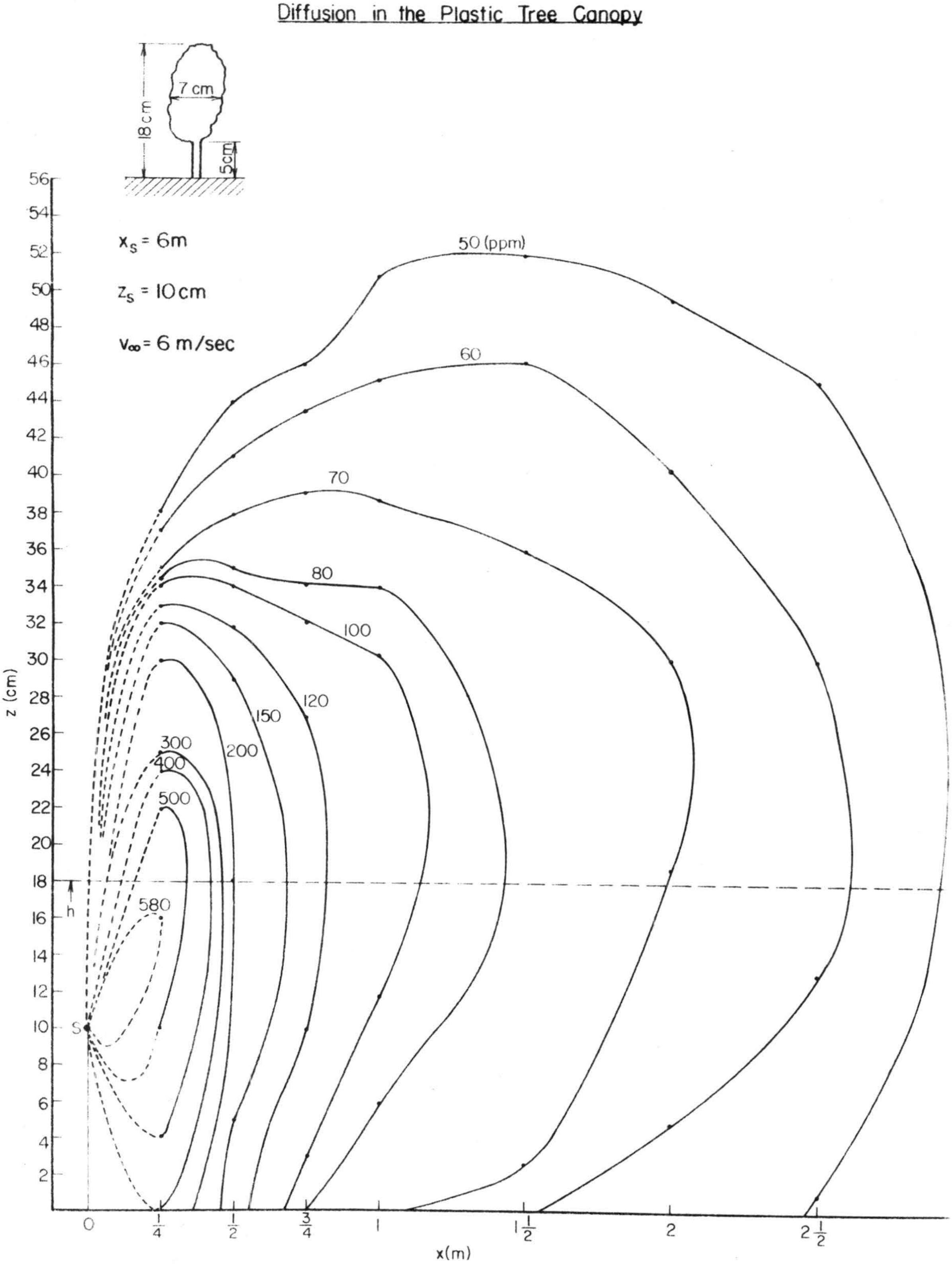

Figure 16a. Diffusion - Isoconcentration profiles.
zs = 10.0 cm

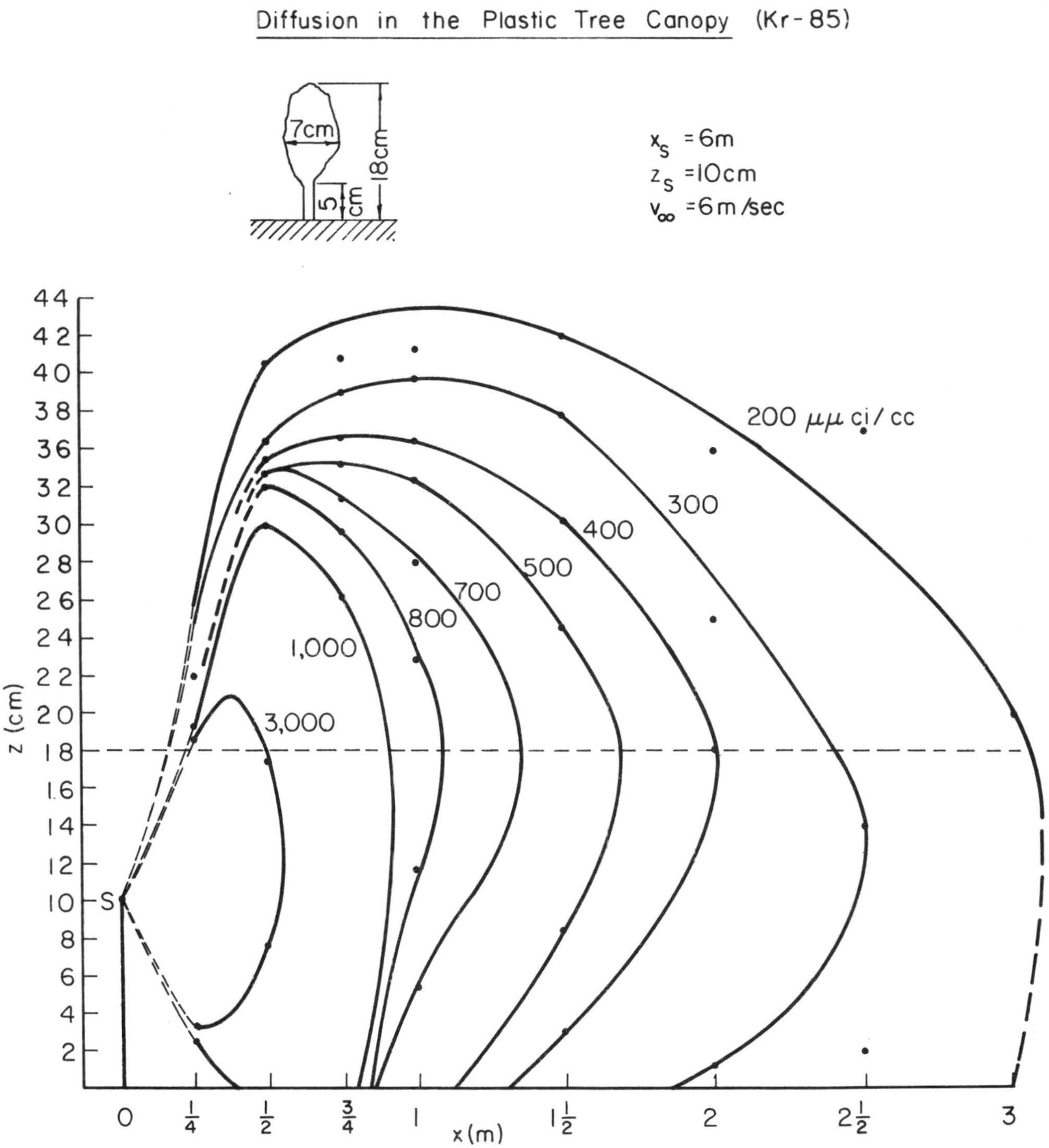

Figure 16b. Diffusion - Isoconcentration profiles.
xs = 6.0 m

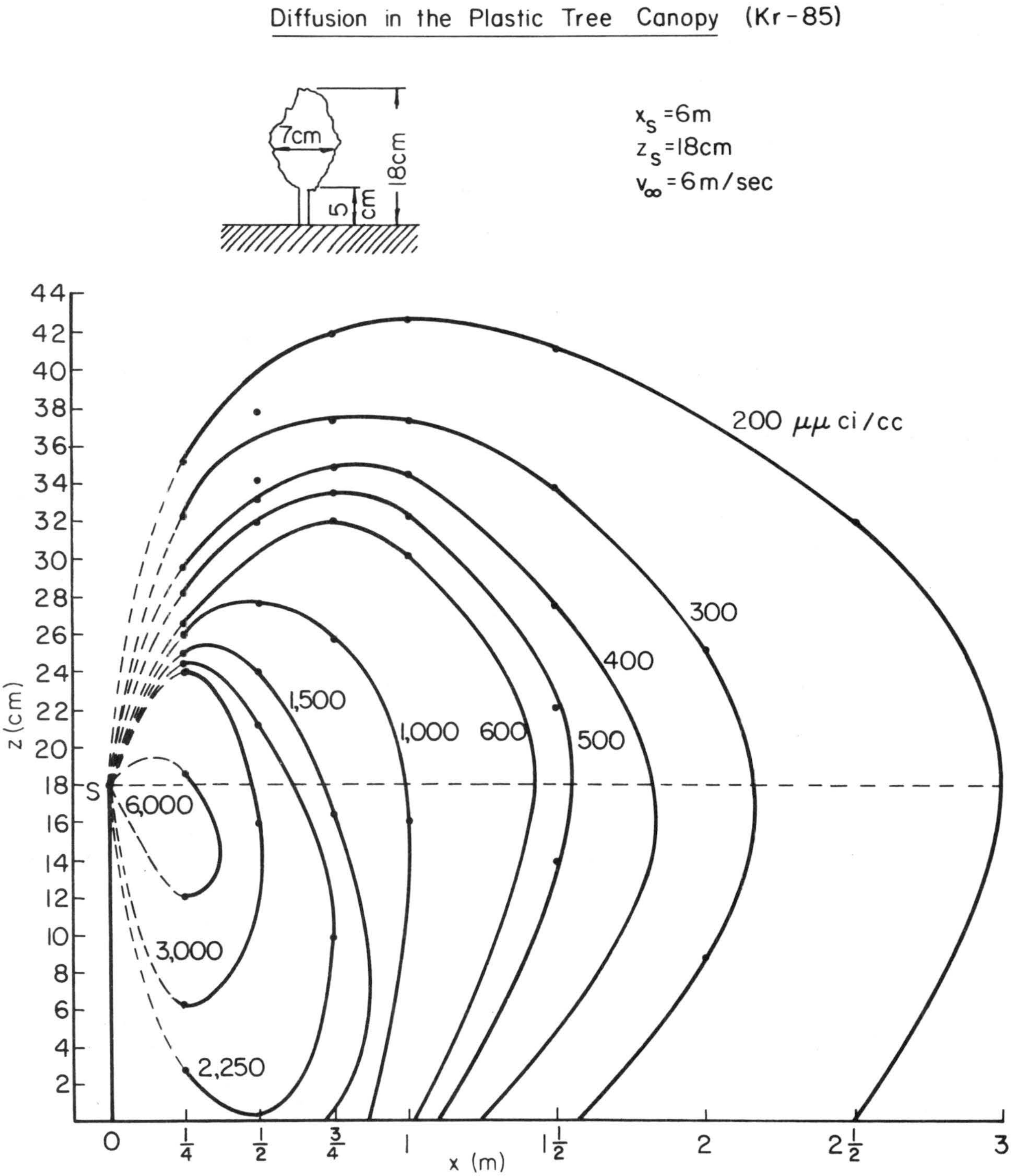

Figure 17. Diffusion - Isoconcentration profiles.
zs = 18.0 cm
xs = 6.0 m

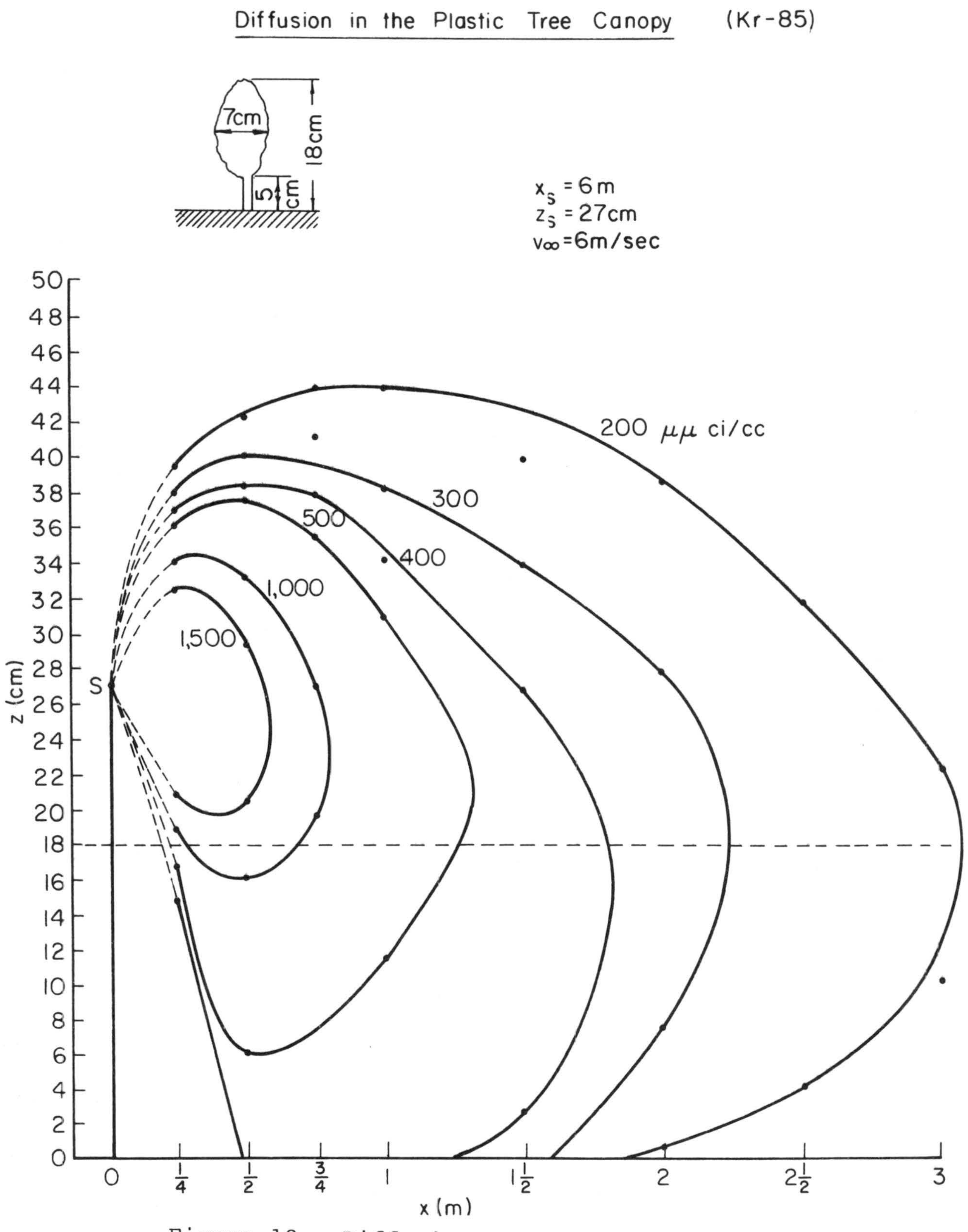

Figure 18. Diffusion - Isoconcentration profiles.
zs = 27 cm
xs = 6.0 m

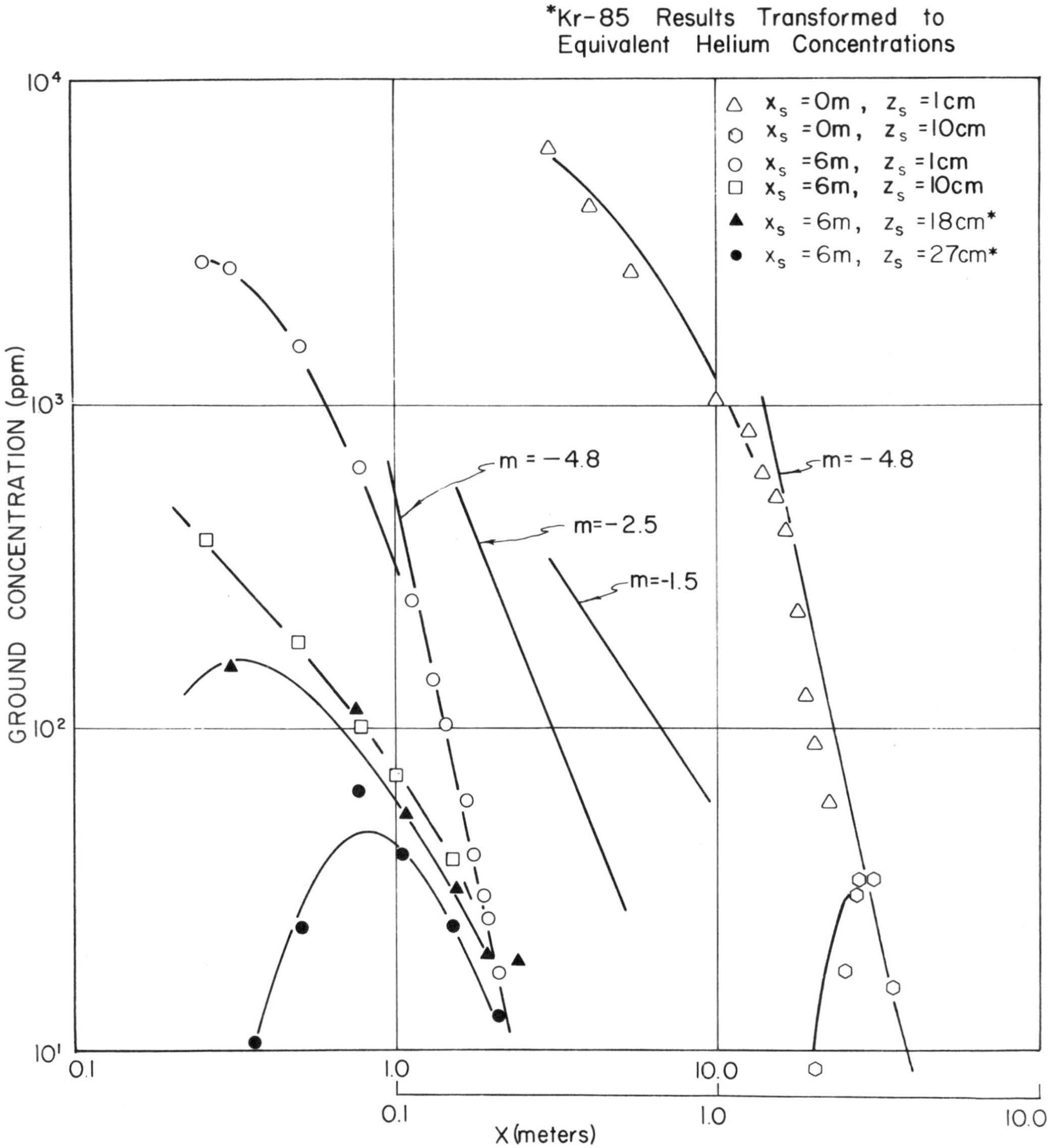

Figure 19. Ground concentration vs downstream distance.

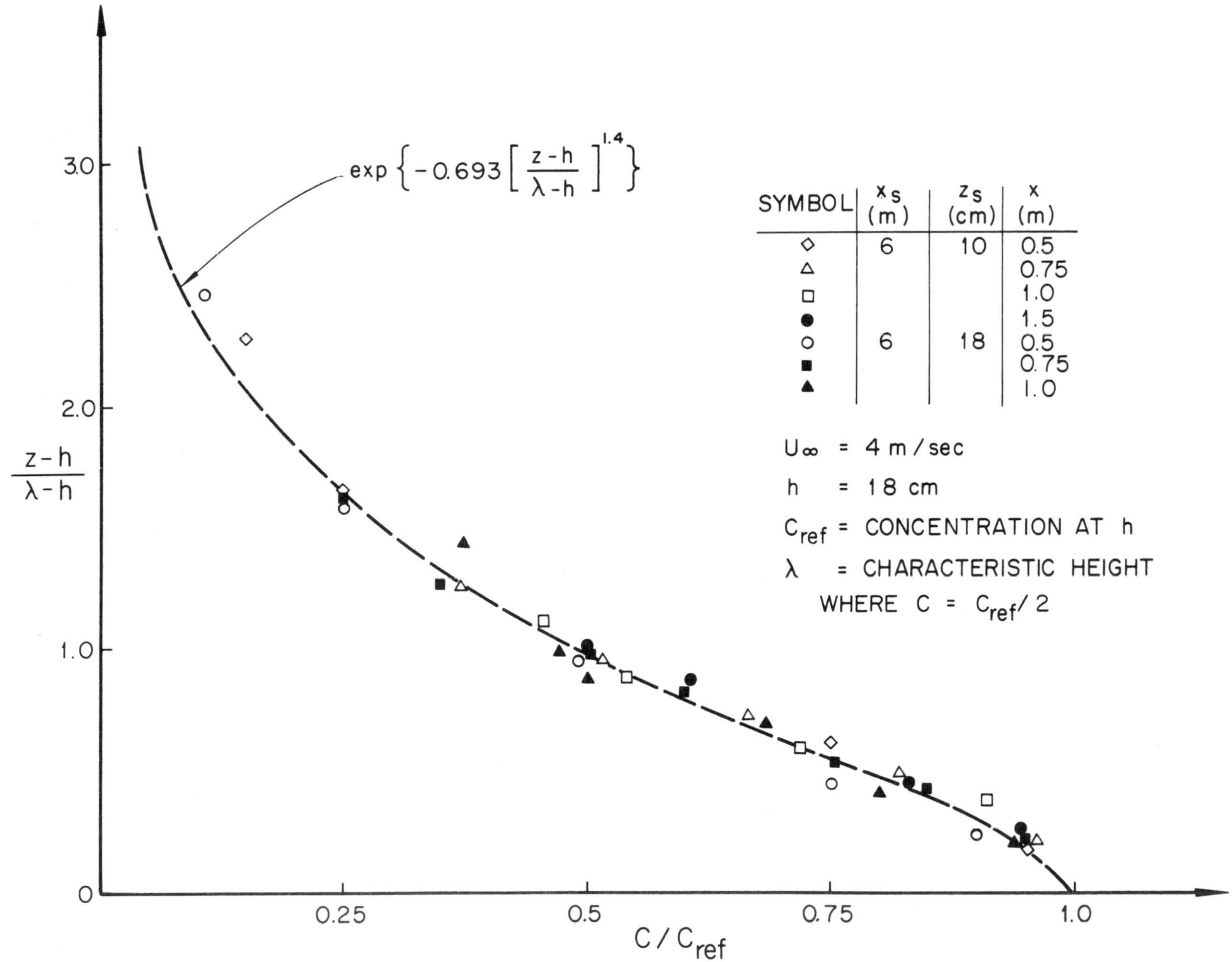

Figure 20. Dimensionless above canopy concentration profiles.

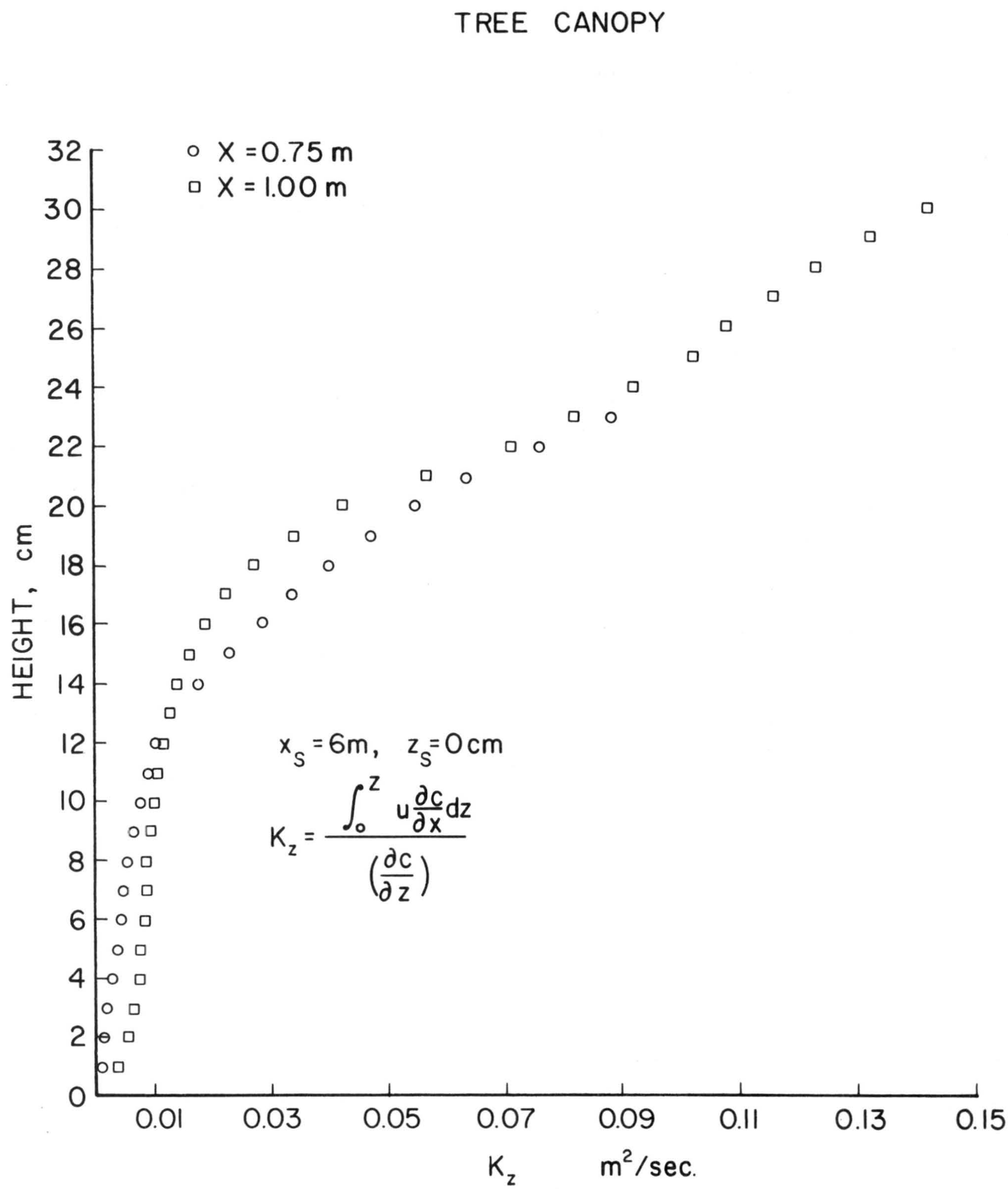

Figure 21. Eddy diffusion coefficient - mass.

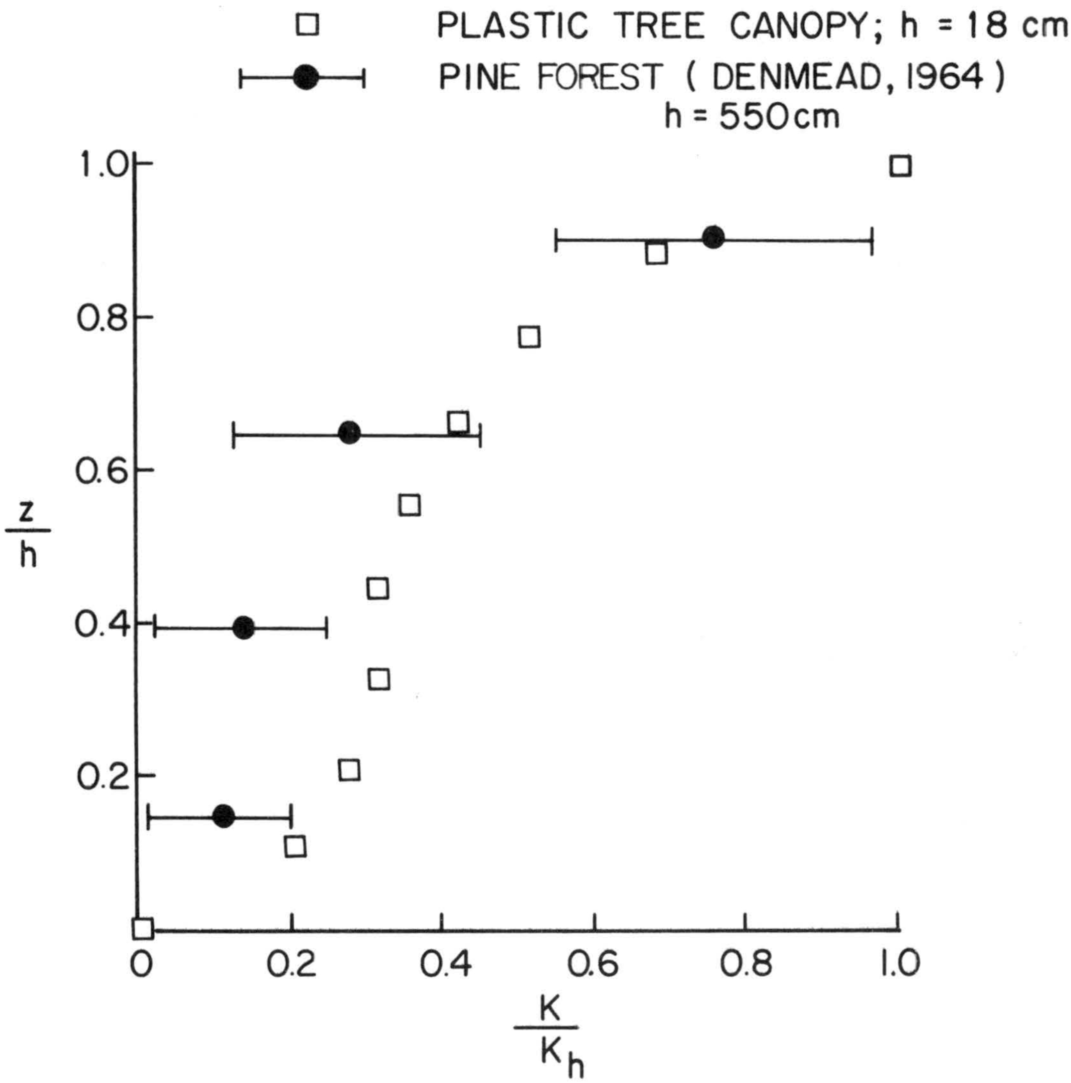

Figure 22. Below canopy dimensionless eddy diffusion coefficient profiles.

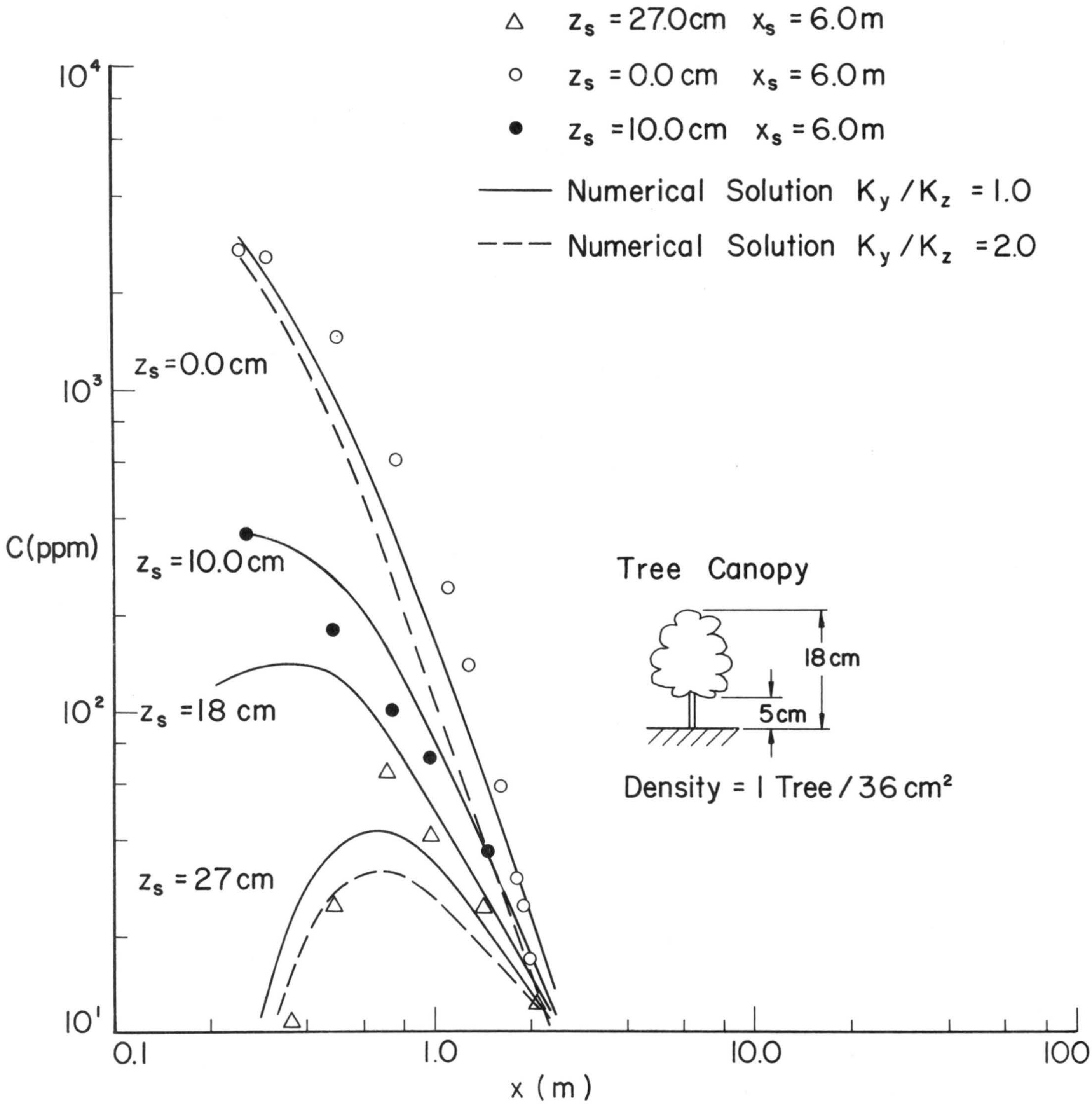

Figure 23. Analytical check on ground concentration variation.

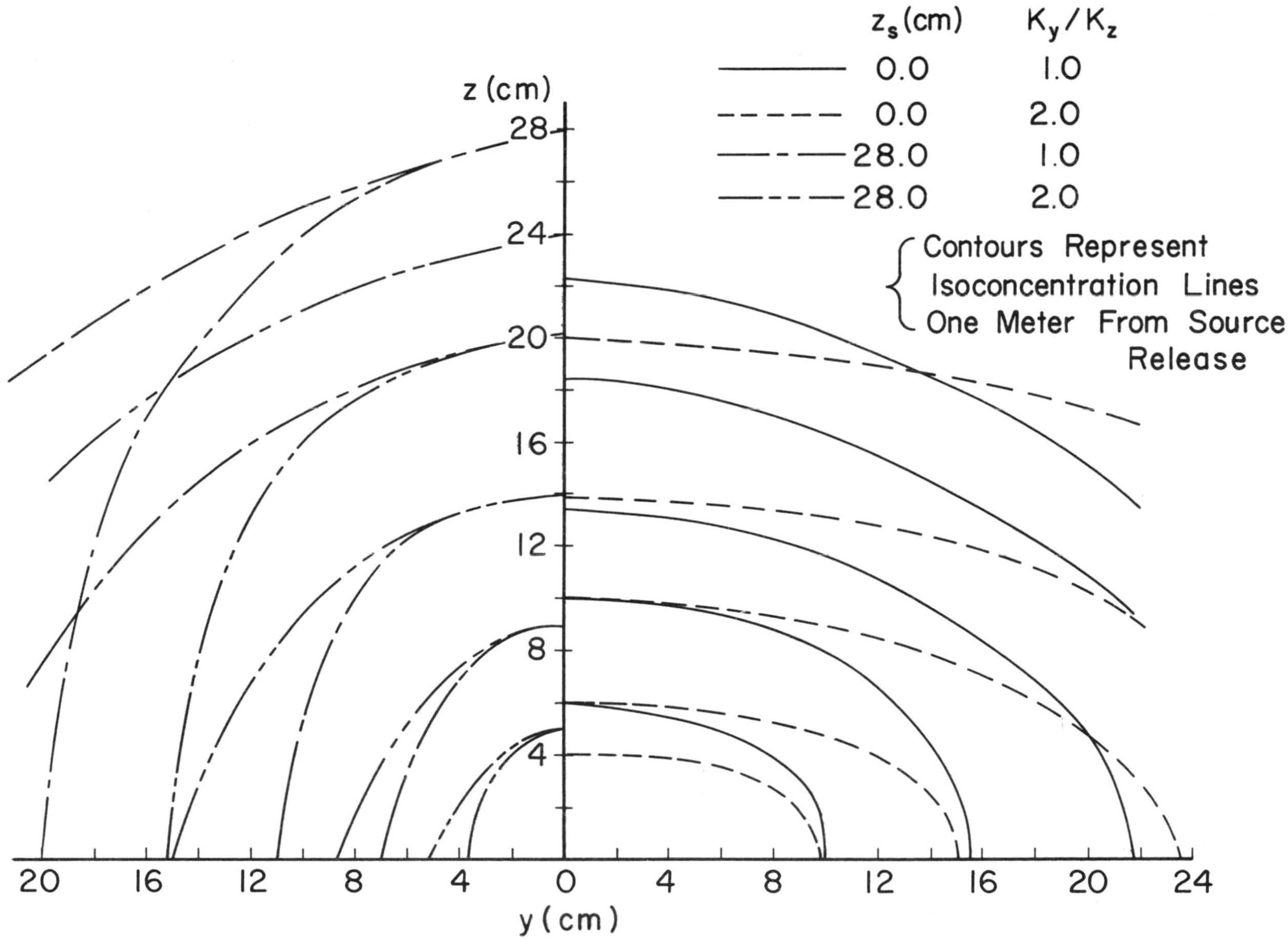

Figure 24. Cross-section-isoconcentration profiles.

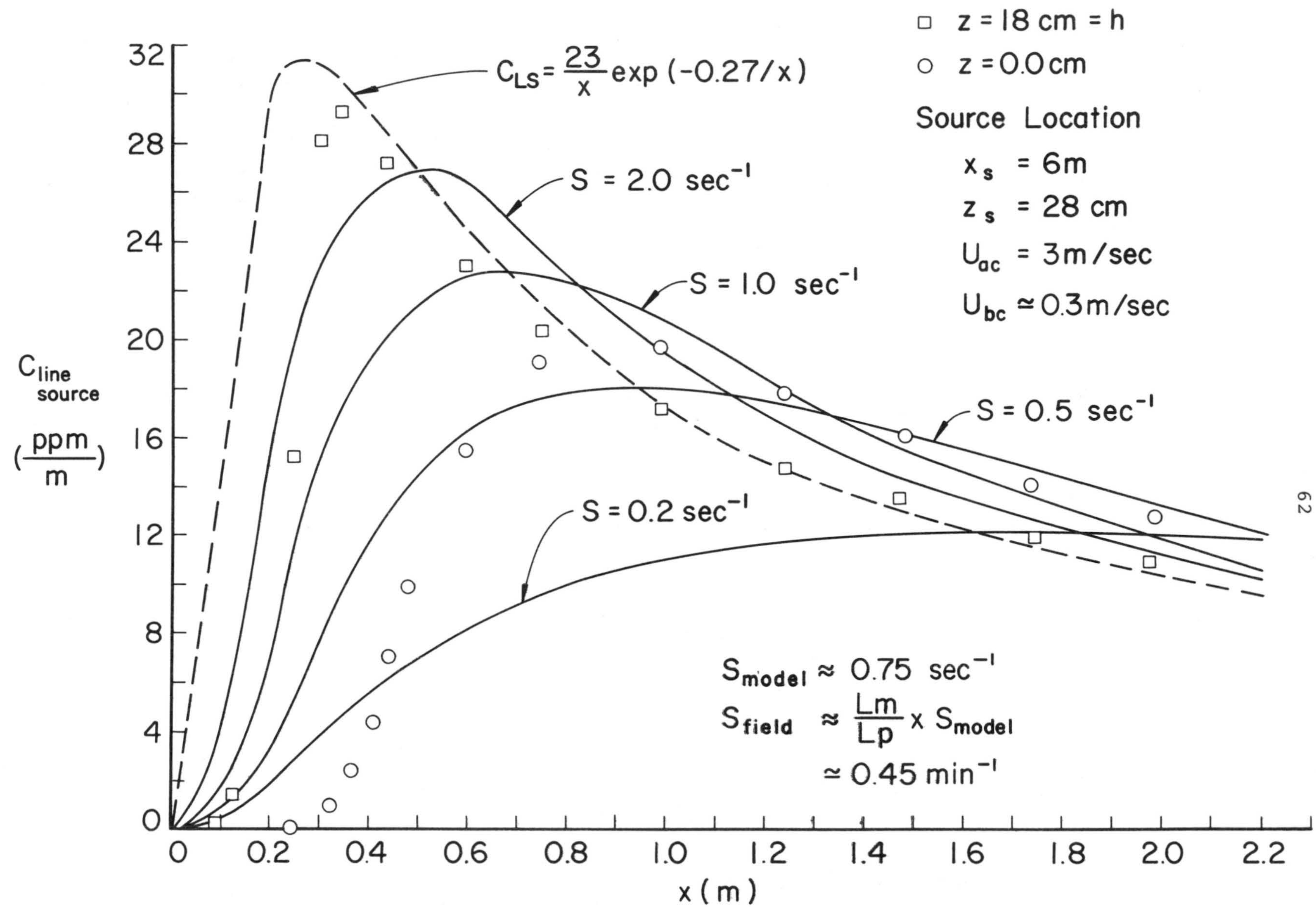

Figure 25. One dimensional penetration model.

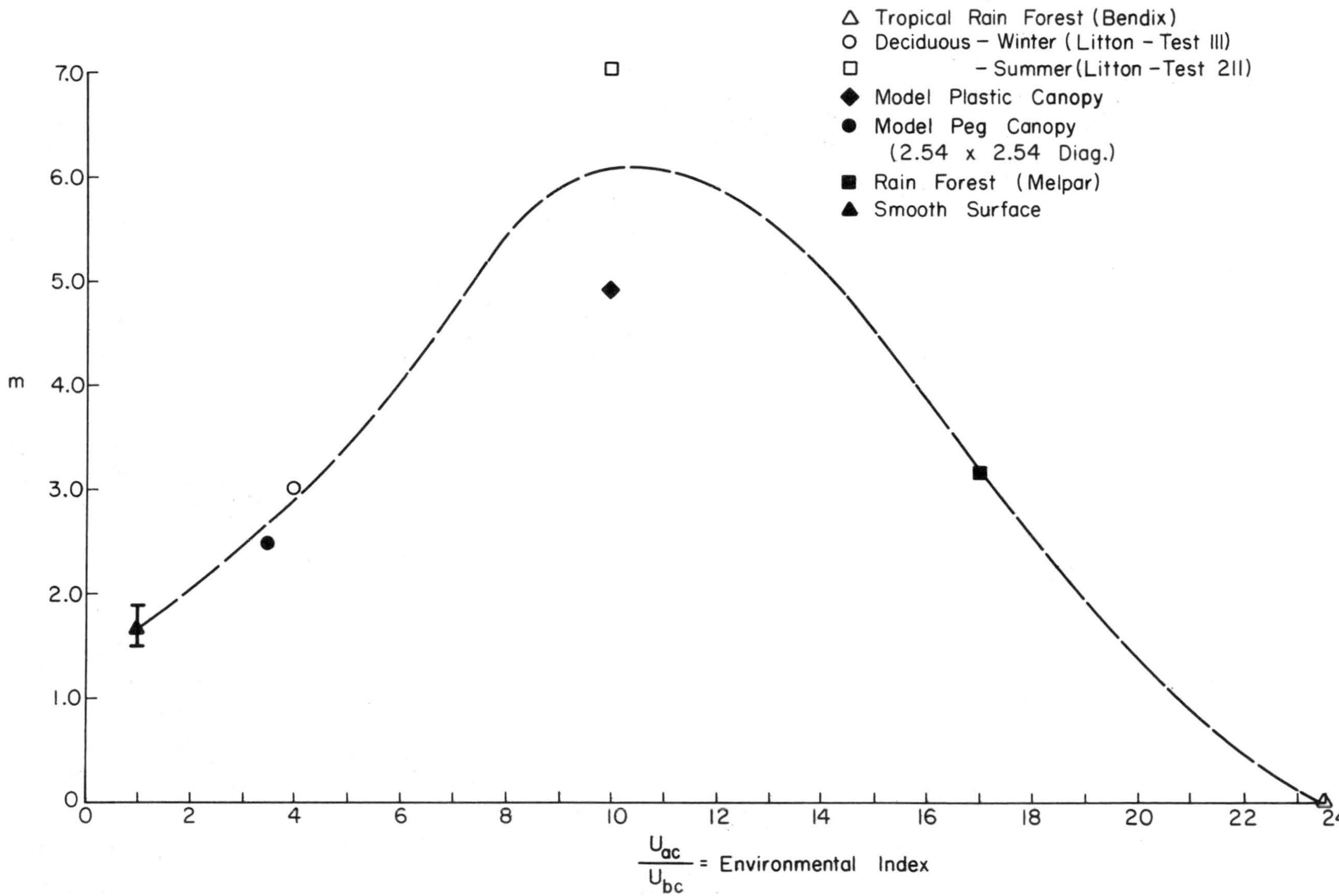

Figure 26. Coefficient m vs environmental index.

Unclassified
Security Classification

DOCUMENT CONTROL DATA - R&D

(Security classification of title, body of abstract and indexing annotation must be entered when the overall report is classified)

1. ORIGINATING ACTIVITY (*Corporate author*)

Colorado State University
Foothills Campus
Fort Collins, Colorado 80521

2a. REPORT SECURITY CLASSIFICATION
Unclassified

2b. GROUP

3. REPORT TITLE

"Wind Tunnel Studies of the Air Flow and Gaseous Plume Diffusion in the Leading Edge and Downstream Regions of a Model Forest"

4. DESCRIPTIVE NOTES (*Type of report and inclusive dates*)

Technical Report

5. AUTHOR(S) (*Last name, first name, initial*)

Meroney, R. N. and Yang, B. T.

6. REPORT DATE	7a. TOTAL NO. OF PAGES	7b. NO. OF REFS
November 1969		49

8a. CONTRACT OR GRANT NO.
DAAB07-68-C-0423

b. PROJECT NO.
1T061102B53A

c.
Task - 17

d.

9a. ORIGINATOR'S REPORT NUMBER(S)
CER69-70RNM-BTY17

9b. OTHER REPORT NO(S) (*Any other numbers that may be assigned this report*)
ECOM-C-0423-6

10. AVAILABILITY/LIMITATION NOTICES

This document has been approved for public release and sale; its distribution is unlimited.

11. SUPPLEMENTARY NOTES

12. SPONSORING MILITARY ACTIVITY

U. S. Army Electronics Command
Atmospheric Sciences Laboratory
Fort Huachuca, Arizona 85613

13. ABSTRACT

A model forest canopy was designed to simulate the meteorological characteristics of typical live forests. Measurements were made of velocity, turbulence, drag, and gaseous plume behavior. Flow properties are compared with recent field measurements. Ground penetration in the initial fetch region results in strikingly different streamline motion as compared to wind motions within the equilibrium regions. Measured values of the vertical eddy diffusion coefficient are shown to predict plume behavior in the equilibrium region very well if a correction is included for the ratio $Ky/Kz > 1.0$.

Ventilation of an elevated line source into the canopy region is compared with a simple one-dimensional model.

DD FORM 1 JAN 64 1473

Unclassified
Security Classification

Unclassified
Security Classification

14. KEY WORDS	LINK A ROLE	LINK A WT	LINK B ROLE	LINK B WT	LINK C ROLE	LINK C WT
Simulation						
Atmospheric Modeling						
Wind-Tunnel Laboratory						
Turbulent Flow						
Diffusion						
Fluid Mechanics						
Micrometeorology						
Forest Meteorology						
Vegetative Canopies						

Unclassified
Security Classification

DISTRIBUTION LIST

DEPARTMENT OF DEFENSE

101 Defense Documentation Center
Attn: DDC-TCA
Cameron Station (Bldg 5)
*20 Alexandria, Virginia 22314

102 Dir. of Defense Research & Engineering
Attn: Technical Library
Rm 3E-1039, The Pentagon
1 Washington, D. C. 20301

103 Joint Chiefs of Staff
Attn: Spec. Asst. Environmental Svcs.
1 Washington, D. C. 20301

106 Defense Intelligence Agency
Attn: DIAAP-10A2
1 Washington, D. C. 20301

108 Director, Defense Atomic Support Agency
Attn: Technical Library
1 Washington, D. C. 20305

DEPARTMENT OF THE NAVY

201 Naval Ships Systems Command
Attn: Code 20526 (Technical Library)
Main Navy Bldg. Rm. 1528
1 Washington, D. C. 20325

205 Director
U. S. Naval Research Laboratory
Attn: Code 2027
2 Washington, D. C. 20390

206 Commanding Officer and Director
U. S. Navy Electronics Laboratory
Attn: Library
1 San Diego, California 92152

207 Commander
U. S. Naval Ordinance Laboratory
Attn: Technical Library
1 White Oak, Silver Spring, Maryland 20910

208 Officer in Charge
Navy Weather Research Facility
Bldg. R-48, Naval Air Station
1 Norfolk, Virginia 23511

210 Commandant, Marine Corps
HQ. U. S. Marine Corps
Attn: Code A04C
1 Washington, D. C. 20380

211 Commandant, Marine Corps
HQ. U. S. Marine Corps
Attn: Code A02F
1 Washington, D. C. 20380

212 Marine Corps Development & Educ. Comd.
Development Cen. Attn: C-E Div.
1 Quantico, Virginia 22134

213 Commander
U. S. Naval Weapons Laboratory
Attn: KXR
1 Dahlgren, Virginia 22448

214 Commander, Naval Air Systems Command
Meteorological Division (Air-540)
1 Washington, D. C. 20360

216 Commander
Naval Weather Service Command
Washington Navy Yard (Bldg. 200)
1 Washington, D. C. 20390

*Increase to 50 copies if releasable to CFSTI. See para 6e(1)(b), ECOMR 70-31, for types of reports not to be sent to DDC.

DEPARTMENT OF THE AIR FORCE

302 Air Force Cambridge Rsch. Labs.
Attn: CREU
L. G. Hanscom Field
1 Bedford, Massachusetts 01730

303 Air Force Cambridge Rsch. Labs.
Attn: CREW
L. G. Hanscom Field
1 Bedford, Massachusetts 01730

304 Air Force Cambridge Rsch. Labs.
Attn: CRH
L. G. Hanscom Field
1 Bedford, Massachusetts 01730

305 Air Force Cambridge Rsch. Labs.
Attn: CRER
L. G. Hanscom Field
1 Bedford, Massachusetts 01730

306 Electronic Systems Div. (ESSIE)
L. G. Hanscom Field
1 Bedford, Massachusetts 01730

307 Electronic Systems Division (ESTI)
L. G. Hanscom Field
2 Bedford, Massachusetts 01730

310 RFCON Central/AVRS.
AF Avionics Laboratory
1 Wright-Patterson AFB, Ohio 45433

311 HQ. AIR Weather Service
Attn: AWVAS/TF (R. G. Stone)
1 Scott Air Force Base, Illinois 62225

312 U. S. Air Force Security Service
Attn: TSG
1 San Antonio, Texas 78241

313 Armament Development & Test Center
Attn: ADBPS-12
1 Eglin Air Force Base, Fla. 32542

314 HQ. Air Force Systems Command
Attn: SCTSE
1 Andrews AFB, Maryland 20331

319 Air Force Weapons Laboratory
Attn: WLIL
1 Kirtland AFB, New Mexico 87117

DEPARTMENT OF THE ARMY

401 OFC of Asst. CH. of Staff for DS-SSS
Department of the Army
Rm. 3C466, The Pentagon
1 Washington, D. C. 20315

402 Asst. Ch. of Staff for Force Development
CRR Nuclear Operations Directorate
Department of the Army
1 Washington, D. C. 20310

405 Ofc. Asst. Sec. of the Army (R&D)
Attn: Asst. for Research
Room 3-E-373, The Pentagon
1 Washington, D. C. 20310

406 Chief of Research and Development
Department of the Army
2 Washington, D. C. 20315

407 Chief of Research and Development
Department of the Army
Attn: CRD/M
1 Washington, D. C. 20310

409 Commanding General
U. S. Army Materiel Command
Attn: AMCMA-EE
1 Washington, D.C. 20315

414 Commanding General
U. S. Army Materiel Command
Attn: AMCRD-TV
1 Washington D. C. 20315

416 Commanding General
U. S. Army Materiel Command
Attn: AMCRD-TV
1 Washington, D. C. 20315

418 Commanding General
U. S. Army Missle Command
Attn: AMSMI-RRA, Bldg. 5429
1 Redstone Arsenal, Alabama 35809

421 CG. U. S. Army Missle Command
Redstone Scientific Info. Center
Attn: Chief, Document Section
3 Redstone Arsenal, Alabama 35809

427 Commanding General
U. S. Army Combat Developments CMD
Combat Support Group
2 Fort Belvoir, Virginia 22060

428 Commanding General
U. S. Army Combat Developments Command
Attn: CDCMR-E
1 Fort Belvoir, Virginia 22060

430 Commanding Officer
USACDC CBR Agency
Attn: Mr. N. W. Bush
1 Fort McClellan, Alabama 36201

432 Commanding Officer
USACDC Artillery Agency
1 Fort Sill, Oklahoma 73503

435 Commanding General
U. S. Army Test & Eval. Command
Attn: AMSTE-EL, -FA, -NBC
3 Aberdeen Proving Ground, Md 21005

436 Commanding General
U. S. Army Test & Eval. Command
Attn: NBC Directorate
1 Aberdeen Proving Ground, Md 21005

437 Commanding General
U. S. Army Munitions Command
Attn: AMSMU-RE-R
1 Dover, New Jersey 07801

438 Commanding General
U. S. Army Munitions Command
Operations Research Group
1 Edgewood Aresenal, MD 21010

439 Commanding General
U. S. Army Munitions Command
Attn: AMSMU-RE-P
1 Dover, New Jersey 07801

442 Commanding Officer
Harry Diamond Laboratories
Attn: Library
1 Washington, D. C. 20438

445 Commanding General
U. S. Army Natick Laboratories
Attn: AMXRF-EG
1 Natick, Mass. 01760

448 Commanding Officer
Picatinny Arsenal
Attn: SMUPA-TV1
1 Dover, New Jersey 07801

449 Commanding Officer
Picatinny Arsenal
Attn: SMUPA-V46, Bldg. 59
2 Dover, New Jersey 07801

453 Commanding Officer
Fort Detrick
Attn: SMUFD-AS-S
1 Frederick, Maryland 21701

(CONTD)

454 Commanding Officer
Fort Detrick
Attn: Tech Library SMUFD-AE-T
1 Frederick, Maryland 21701

459 Commanding Officer
Edgewood Arsenal
Attn: SMUEA-TSTI-TL
1 Edgewood Arsenal, Maryland 21010

460 Commanding Officer
U. S. Army Nuclear Defense Lab.
Attn: Library
2 Edgewood Arsenal, Maryland 21010

463 President
U. S. Army Artillery Board
1 Fort Still, Oklahoma 73503

464 Commanding Officer
Aberdeen Proving Ground
Attn: Technical Library, Bldg. 313
2 Aberdeen Proving Ground, Md. 21005

469 Commanding Officer
U. S. Army Ballistics Rsch. Labs.
Attn: Tech. Info. Div.
1 Aberdeen Proving Ground, Md. 21005

470 Commanding Officer
U. S. Army Ballistic Research Labs.
Attn: AMXBR-B & AMXBR-1A
2 Aberdeen Proving Ground, Md. 21005

472 Commanding Officer
U. S. Army Limited Warfare Lab.
Attn: CRDLWL-7C
1 Aberdeen Proving Ground, Md. 21005

475 Commanding Officer
USA Garrison
Attn: Technical Reference Div.
1 Fort Huachuca, Arizona 85613

483 Commander
U. S. Army Research Office (Durham)
Box CM-Duke Station
1 Durham, North Carolina 27706

488 USA Security Agcy. Combat Dev. Actv.
Attn: IACDA-P(T) and IACDA-P(L)
Arlington Hall Station, Bldg. 420
2 Arlington, Virginia 22212

489 U. S. Army Security Agcy. Proc. Ctr.
Attn: TAVAPC-R&D
Vint Hill Farms Station
1 Warrenton, Virginia 22186

490 Technical Support Directorate
Attn: Technical Library
Bldg. 3330
1 Edgewood Arsenal, Maryland 26010

491 Commandant
U.S. Army Chemical Center & School
Micrometeorological Section (Chem. Br.)
1 Fort McClellan, Alabama 36201

492 Commandant
U.S. Army Air Defense School
Attn: C&S Dept. MSL Sci. Div.
1 Fort Bliss, Texas 79916

493 Director
U.S.A. Engr. Waterways Exper. Station
Attn: Research Center Library
2 Vicksburg, Mississippi 39180

495 CG, Deseret Test Center
Attn: STEDO-TT-ME(S) MET Div.
Bldg. 103, Soldiers Circle
1 Fort Douglas, Utah 84113

496 Commanding General
USA CDC Combat Arms Group
1 Ft. Leavenworth, Kansas 66027

497 Commanding Officer
USA Aviation Materiel Lab.
Attn: Technical Director
1 Fort Eustis, Virginia 23604

503 Director
U. S. Army Advanced Matl. Conc. Agcy.
Attn: AMXAM
1 Washington, D.C. 20315

596 Commanding Officer
U. S. Army Combat Dev. Command
Communications-Electronics Agency
1 Fort Monmouth, New Jersey 07703

597 Commandant
U.S. Army Signal School
Attn: Meteorological Department
1 Fort Monmouth, New Jersey 07703

U.S. ARMY ELECTRONICS COMMAND

*604 U. S. Army Liaison Office
MTT. Bldg. 26, Rm. 131
77 Massachusetts Avenue
1 Cambridge, Mass. 02139

605 U. S. Army Liaison Office
MTT-Lincoln Laboratory, Rm. A-210
P. O. Box 73
1 Lexington, Mass. 02173

606 Headquarters
U.S. Army Combat Dev. Command
Attn: CDCLN-EL
1 Fort Belvoir, Virginia 22060

607 Commanding General
U.S. Army Tank-Automotive Command
Attn: AMSTA-Z, Mr. R. McGregor
1 Warren, Michigan 48090

608 USAECOM Liaison Ofc., Stanford Univ.
Solid State Electronics Lab. McCul. Bldg.
1 Stanford, California 94305

613 Chief, Atmos. Sciences Res. Div.
ASL, USAECOM, Attn: AMSEL-BL-RD
1 Fort Huachuca, Arizona 85613

680 Commanding General
U.S. Army Electronics Command
Fort Monmouth, N. J. 07703

1 AMSEL-EW
1 AMSEL-ME-NMP-PS
2 AMSEL-TD-TI
1 AMSEL-RD-MT
1 AMSEL-XL-D
1 AMSEL-NL-D
1 AMSEL-VL-D

*Unclassified, unlimited reports only.
**Or number specified in contract. Add COTR's mail symbol

(5) Commanding Officer
Atmospheric Sciences Lab.
US Army Electronics Command
White Sands Missile Range, N.M. 88002

OTHER RECIPIENTS

504 Commanding General
U. S. Army Materiel Command
Attn: AMCRD-R (H. Cohen)
1 Washington, D.C. 20315

702 Institute of Science and Tech.
The University of Michigan
P. O. Box 618, (Iria Library)
1 Ann Arbor, Michigan 48107

703 NASA Scientific & Tech. Info. Fac.
Attn: Acquisitions Branch (S-AK/DL)
P. O. Box 33
2 College Park, Maryland 20740

707 Target Signature Analysis Cen.
Willow Run Labs-Inst. of Sci & Tech.
Univ. of Michigan, P. O. Box 618
1 Ann Arbor, Michigan 48107

709 Battelle-Defender Info. Center
Battelle Memorial Institute
505 King Avenue
1 Columbus, Ohio 43201

714 Infrared Information & Analysis Center
University of Michigan
Inst. of Science and Tech.
Box 618,
1 Ann Arbor, Michigan 48107

721 Vela Seismic Info. Center
University of Michigan
Box 618
3 Ann Arbor, Michigan 48107

Note: Distribute only unclassified reports to the following addresses. Consider intent of distribution statement.

901 Head, Atmospheric Sciences Sect.
National Science Foundation
1800 G. Street, N.W.
1 Washington, D.C. 20550

902 Director, Systems R&D Service
Federal Aviation Administration
800 Independence Ave., S.W.
1 Washington, D.C. 20590

903 Atmospheric Sciences Library
Environmental Science svcs Admin.
1 Silver Spring, Maryland 20910

904 Div. of Meteorology & National
c/o Air Pollution Control Admin.
3820 Merton Drive
1 Raleigh, N.C. 27609

905 U. S. Department of Agriculture
Attn: William A. Main
University of Minnesota
1 St. Paul, Minnesota 55101

907 Chief, Fallout Studies Branch
Div. of Biology and Medicine
Atomic Energy Commission
1 Washington D.C. 20545

908 NASA Headquarters
Meteorology & Sounding Br. (Code SAM)
Space Applications Programs
1 Washington, D. C. 20546

910 Director
Atmospheric Physics & Chem. Lab R31
ESSA-Department of Commerce
1 Boulder, Colorado 80302

911 Natl. Center for Atmospheric Res.
NCAR Library, Acquisitions-Reports
1 Boulder, Colorado 80302

912 OCE, Bureau of Reclamation
Attn: D755, Bldg. 67
1 Denver, Colorado 80225

913 National Oceanographic Data Cen.
Code 2220
Bldg. 160, WNY
1 Washington, D. C. 20390